

Faculteit Industriële Ingenieurswetenschappen

master in de industriële wetenschappen: chemie

Masterthesis

Characterization of micromixing in batch and SSE reactor for high viscous systems

Valerio Cosemans

Scriptie ingediend tot het behalen van de graad van master in de industriële wetenschappen: chemie

PROMOTOR :

Prof. dr. ir. Leen THOMASSEN

BEGELEIDER :

De heer Jonas LONCKE

Gezamenlijke opleiding UHasselt en KU Leuven



Universiteit Hasselt | Campus Diepenbeek | Faculteit Industriële Ingenieurswetenschappen | Agoralaan Gebouw H - Gebouw B | BE 3590 Diepenbeek

Universiteit Hasselt | Campus Diepenbeek | Agoralaan Gebouw D | BE 3590 Diepenbeek
Universiteit Hasselt | Campus Hasselt | Martelarenlaan 42 | BE 3500 Hasselt



2023
2024

Faculteit Industriële Ingenieurswetenschappen

master in de industriële wetenschappen: chemie

Masterthesis

Characterization of micromixing in batch and SSE reactor for high viscous systems

Valerio Cosemans

Scriptie ingediend tot het behalen van de graad van master in de industriële wetenschappen: chemie

PROMOTOR :

Prof. dr. ir. Leen THOMASSEN

BEGELEIDER :

De heer Jonas LONCKE



KU LEUVEN

Preface

It is with great pleasure that I present my master's thesis "Characterization of micromixing in batch and single-screw extrusion reactor". This thesis was written over the course of four months to be eligible for the degree of master of Chemical engineering technology. Throughout my childhood and academic career, I have always been curious about how and why things work the way they do, but also enjoyed building and thinking. Therefore, an internship at CIPT was evident. I had a great time doing research surrounded by people that allowed me to thrive. Besides, the technical expertise that I gained, I have learned to appreciate the necessity of time management, stress resistance, resilience and perseverance. I would like to thank my promotor Prof. Thomassen for her supervision during the writing of this thesis but also for her straightforwardness during our meetings. Second, I would like to thank Jonas Loncke for his excellent supervision during lab work. It was an honor to work beside you and contribute to your PhD thesis. Lastly, I would like to thank my parents and siblings for their support.

Table of Contents

| | |
|--|----|
| List of Tables | 5 |
| List of Figures | 7 |
| Abstract..... | 9 |
| Abstract in Dutch..... | 11 |
| 1 Introduction..... | 13 |
| 2 Literature study | 15 |
| 2.1 Reactive extrusion and mechanochemistry..... | 15 |
| 2.1.1 Applications | 15 |
| 2.1.2 Challenges..... | 16 |
| 2.2 Macromixing and micromixing | 17 |
| 2.3 Experimental determination of micromixing efficiency | 18 |
| 2.3.1 Methods of studying micromixing efficiency | 18 |
| 2.3.2 The Villiermaux-Dushmann method | 18 |
| 2.4 Villiermaux-Dushmann method used in batch experiments | 20 |
| 2.4.1 Determination of the chemical system | 20 |
| 2.4.2 Effect of the reactor dimensions | 21 |
| 2.4.3 Effect of injection time on micromixing efficiency..... | 21 |
| 2.4.4 Effect of the rotation speed of the impeller on micromixing efficiency | 22 |
| 2.4.5 Effect of backmixing in tubing on micromixing efficiency..... | 23 |
| 2.4.6 Mixing experiments in viscous media | 23 |
| 2.5 Villiermaux-Dushmann method used in flow experiments | 25 |
| 3 Materials and Methods | 27 |
| 3.1 Triiodide quantification..... | 27 |
| 3.1.1 Villiermaux-Dushmann method: Triiodide formation | 27 |
| 3.1.2 Analytical method: UV-VIS spectroscopy | 27 |
| 3.2 Mixing experiments | 27 |
| 3.2.1 Preparation of solutions | 27 |
| 3.2.2 Batch experiments..... | 28 |
| 3.2.3 Flow experiments | 29 |
| 4 Results | 31 |
| 4.1 Batch experiments in OptiMax reactor..... | 31 |
| 4.1.1 Aqueous medium | 31 |
| 4.1.2 Viscous medium $\eta = 100 \text{ mPa}\cdot\text{s}$ | 32 |
| 4.1.3 Sub-conclusion..... | 34 |
| 4.2 Flow experiments in Single-screw extrusion reactor..... | 34 |
| 4.2.1 Optimization of flow rate ratio R..... | 34 |

| | | |
|-------|--|----|
| 4.2.2 | Variation of mixing element type | 35 |
| 4.2.3 | Variation of screw configuration | 36 |
| 4.2.4 | Sub-conclusion..... | 37 |
| 5 | Conclusion | 39 |
| | References..... | 41 |

List of Tables

| | |
|--|----|
| Table 1: Summary of different regimes based on the relative value of t_m and t_r | 17 |
| Table 2: Different options for studying micromixing | 18 |
| Table 3: Buffer composition for aqueous solutions (Volume = 5 l)..... | 20 |
| Table 4: Composition of the stock solution (100 ml)..... | 27 |
| Table 5: Composition of acid and buffer solution for mixing experiments | 28 |
| Table 6: Parameter ranges (Batch). | 28 |
| Table 7: Stirring speed sweeps at different injection flow rates..... | 29 |
| Table 8: Parameter ranges (flow). | 29 |
| Table 9: Optimization of ratio R for flow experiments. | 30 |
| Table 10: Stirring speed sweeps for flow experiments | 30 |

List of Figures

| | |
|--|----|
| Figure 1: Different mixing elements studied in this thesis | 13 |
| Figure 2: Sections of single screw(left) and twin screw (right) extrusion reactor with 1=input, 2=feed, 3=reaction center, and 4=output | 15 |
| Figure 3: Several organic syntheses performed in the SSE setup | 16 |
| Figure 4: Different combinations macromixing and micromixing regimes | 18 |
| Figure 5: Influence of injection time on micromixing efficiency | 21 |
| Figure 6: Segregation indexes between different injections inside the same batch reactor (Parameter α is the micromixedness factor which is proportional to the segregation index X_s) | 22 |
| Figure 7: Effect of stirring speed on micromixing efficiency with $\omega_{crit} = 1200$ rpm | 22 |
| Figure 8: Effect of back mixing of micromixing efficiency | 23 |
| Figure 9: Effect of pipe internal diameter on back mixing and micromixing efficiency | 23 |
| Figure 10: Effect of injection time of micromixing efficiency in viscous medium of 170 mPa·s. The data points were received through mixing experiments in a 1 l stirred tank reactor | 24 |
| Figure 11: The influence of stirring speeds N on the micromixedness ratio a for different concentrations of HEC hence different viscosities | 24 |
| Figure 13: Batch setup | 28 |
| Figure 14: Flow experiment setup | 29 |
| Figure 15: Optimization of injection time in OptiMax reactor for aqueous solutions | 31 |
| Figure 16: Stirring speeds sweep in OptiMax reactor for aqueous solutions | 32 |
| Figure 17: Titration curve of buffer solution with 83 m% glycerol (100 mPa·s) | 32 |
| Figure 18: Optimization of injection time in OptiMax reactor (100 mPa·s) | 33 |
| Figure 19: Stirring speed sweep in OptiMax reactor (100 mPa·s) | 33 |
| Figure 20: Micromixing efficiency in OptiMax reactor (Aqueous vs 100 mPa·s solution) | 34 |
| Figure 21: Optimization of flow rate R for normal pin mixer in aqueous solution | 35 |
| Figure 22: Effect of mixing elements types in aqueous and 100 mPa·s solutions for $R = 125$ | 35 |
| Figure 23: CFD simulations for mixing in screw reactor | 36 |
| Figure 24: Effect of screw configuration on micromixing efficiency | 37 |

Abstract

In chemical processes, optimal mass transfer is necessary to ensure high reaction kinetics. Mass transfer is enhanced through efficient micromixing, which reduces the diffusion path length of reagents. Mixing is facilitated through the use of solvents, but using solvents often necessitates separation steps and causes waste streams. Therefore, solvent-free process intensification is desired. However, due to the increasing viscosity, using less solvents complicates flow processes. Single-screw extrusion reactors can overcome this challenge although mixing is often suboptimal. Therefore, this thesis investigates if using a single-screw reactor implemented with specialized mixing elements can enhance micromixing.

The goal of this master's thesis is to characterize micromixing in a single-screw extrusion reactor for aqueous solutions and viscous solutions of up to 100 mPa·s. The Villermaux-Dushman method is used to characterize micromixing at different stirring speeds and injection flow rates. Additionally, different mixing elements namely Normal pin and Saxton, and different screw configurations are studied to optimize micromixing.

This thesis shows that increasing viscosity adversely affects micromixing efficiency for both batch and single-screw reactors. Moreover, Saxton mixing elements provide the most efficient micromixing for 1 mPa·s and 100 mPa·s media. Additionally, variations of screw configuration have no significant effect on micromixing efficiency.

Abstract in Dutch

Binnen chemische processen is een optimale massaoverdracht noodzakelijk om een hoge reactiekinetiek te garanderen. Efficiënte micromenging verbetert massaoverdracht door de diffusiepadlengte van reagentia te verminderen. Het mengen wordt vergemakkelijkt door het gebruik van solventen, maar brengt extra scheidingsstappen en extra afvalstromen met zich mee. Solvent-vrije procesintensificatie dringt zich dus op, maar de toenemende viscositeit vormt een uitdaging aangezien deze de menging bemoeilijkt. Single-screw extrusiereactoren kunnen deze uitdaging overwinnen, hoewel de menging vaak suboptimaal is. Daarom onderzoekt deze thesis of het gebruik van een schroefreactor, uitgerust met gespecialiseerde mengelementen, de micromenging kan verbeteren.

Het doel van deze thesis is het karakteriseren van micromenging in een schroefreactor voor waterige oplossingen en viskeuze oplossingen tot 100 mPa·s. De Villermaux-Dushman-methode wordt gebruikt om micromenging bij verschillende roersnelheden en injectiedebieten te karakteriseren. Daarnaast worden verschillende mengelementen, namelijk Normal pin en Saxton, en verschillende schroefconfiguraties bestudeerd om micromenging te optimaliseren.

Deze thesis toont aan dat het verhogen van de viscositeit een negatieve invloed heeft op de micromengefficiëntie in zowel batch- als schroefreactor. Verder bieden Saxton-mengelementen de meest efficiënte micromenging voor mengsels van 1 mPa·s en 100 mPa·s. Daarnaast heeft de schroefconfiguratie geen significant effect op de micromengefficiëntie.

1 Introduction

The Centre for Industrial Process Technology (CIPT) focuses on developing and implementing novel technology in existing chemical or biochemical processes. The research group is involved in projects studying crystallization, distillation, microencapsulation, dispersion, and chemical synthesis [1]. In addition, the group specializes in reactor characterization in which techniques such as residence time distribution and the Villermaux-Dushman method are employed to study macro- and micromixing performance, respectively.

The study of mixing both at the macro- and microscale is a cornerstone of the development of more sustainable chemical processes. Chemical processes often use solvents to enhance mass transfer but also act as a heat sink through effective mixing which reduces the diffusion path length of reagents. Effective micromixing corresponds to higher reaction kinetics, selectivity, and product distribution [2], [3]. However, the use of solvents often necessitates separation steps and causes waste streams. Furthermore, using solvents in industrial chemical processes contributes up to 90% to the total carbon footprint of the process [4]. Therefore, solvent-free process intensification has gained increasing interest as a way towards more green chemistry. However, using no solvents complicates flow processes due to the increasing viscosity which in turn complicates efficient micromixing.

Increasing viscosity is a known problem within polymer processing. However, the polymer sector has overcome this challenge through the use of screw extruders. In extruders, reagents are transported and mixed through the reactor by rotary motion of a screw. This screw motion assists in applying large shear forces which help to break up the fluid and thus overcome high viscosities. The screw always contains transporting elements and mixing elements. Mixing elements have peculiar geometric patterns that disturb the flow path and promote macromixing. Micromixing has not been studied in literature. Expanding this technology to other branches of the chemical industry is evident. However, the implementation of liquid/liquid and liquid/solid chemical synthesis in extrusion reactors is still challenging because it often results in the formation of byproducts and lower reaction kinetics compared to reactions in solution due to suboptimal mixing efficiency [5].

Therefore, this thesis will investigate if the use of special mixing elements can enhance micromixing inside a single-screw extrusion reaction. To study micromixing, the Villermaux-Dushman method is used which has been studied extensively for aqueous solutions as opposed to viscous solutions. Therefore, preliminary batch experiments will serve as a benchmark for flow experiments. Figure 1 shows the two types of mixing elements that are investigated in this thesis namely Saxton and Normal pin.



Figure 1: Different mixing elements studied in this thesis [6]

The overall goal of this thesis is to characterize micromixing for a single screw extrusion reactor. To reach that goal, several objectives have to be met. The first objective is to determine which mixing element enhances micromixing the most for both aqueous and 100 mPa·s solutions. Second, the effect of screw configuration on micromixing efficiency is investigated for both aqueous and 100 mPa·s solutions. Three screw configurations are tested specifically M-T-M, M-T-T and M-T-M* respectively, with M = mixing element and T = transport element.

2 Literature study

2.1 Reactive extrusion and mechanochemistry

Extruding is a forming technique primarily used in the polymer industry in which a deformable material is pressed through a die, for example, in the production of pipes and Teflon tubing. The deformable material is subjected to high temperature, pressure, and mechanical forces which pave the way for mechanochemistry inside extruders. Figure 2 shows the general parts of an extruder [5].

Extrusion reactors are extruders that are used as a continuous chemical reactor. Reactants are fed into the reactor as either a solid or a liquid after which the mixture is led to the reaction center of the reactor. In this region, matter is axially displaced towards the reactor outlet and simultaneously mixed radially by the rotary motion of a screw. During their displacement, the reactants are allowed to mix and are subjected to mechanical stresses and high temperatures that activate chemical reactions. These mechanochemical reactions are promising candidates for more sustainable processes. In theory, no solvents are needed for these reactions but in practice, the use of solvents is often limited to liquid-assisted grinding (LAG) agents and glidants namely sand or sodium chloride that facilitate flow and reaction progression in the reactor [7], [8], [9], [10].

Figure 2 shows the two types of extruders namely single screw extruders (SSE) and twin screw extruders (TSE). SSEs are easy to use and are cheaper than TSEs. However, SSEs lag in terms of mixing efficiency because of the interlocking of the screws in TSEs which facilitates more intimate mixing. SSE is more versatile than TSE because the implementation of different EME-types is not limited by the requirement of interlocking [11].

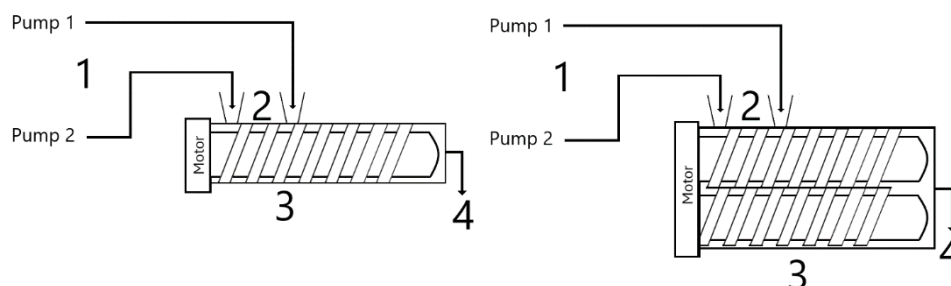


Figure 2: Sections of single screw(left) and twin screw (right) extrusion reactor with 1=input, 2=feed, 3=reaction center, and 4=output [5]

2.1.1 Applications

The reactive extrusion process is widely used in the polymer industry because it offers an efficient method of altering polymers with chosen characteristics for example, improved thermal stability, mechanical strength, and chemical resistance. One of the key advantages of reactive extrusion is its ability to achieve a high conversion within a short residence time. The continuous nature of the extrusion process ensures that the reaction proceeds rapidly and uniformly, resulting in a homogeneous polymer product. Additionally, reactive extrusion offers better control over reaction conditions, such as temperature, pressure, and residence time, which allows for optimizing reaction kinetics and producing polymers with specific properties. This versatility makes reactive extrusion a valuable tool in the polymer industry, enabling the development of innovative materials for various applications, including the automotive, aerospace, packaging, glues, and electronics sectors [7], [12].

The pharmaceutical industry could also benefit from advances made in reaction extrusion and mechanochemistry. The first research articles on mechanochemistry done in twin screw extruder reactors were published in 2017 and since then several organic reactions have been performed through

mechanochemical means such as the Wittig reaction, Michael addition, Aldol condensation, and the synthesis of MOFs [7], [8], [9], [13]. Figure 3 shows several organic synthesis reactions performed SSE-setup performed by [14]. Remarkable is the high yield that was acquired for several reactions, for example, the Sudan dye synthesis (A) and Knoevenagel condensation (B) which got a yield of 95% and 97% respectively. In addition, the reaction time is significantly shorter for single screw extrusion in comparison to an ordinary reaction in solution. For example, by using single screw extrusion for alcohol oxidation (C) the reaction time was lowered by 99.6% (from 4 hours in batch solution to 1 minute in flow extrusion) while producing product with the same yield namely 93% on 10 g scale.

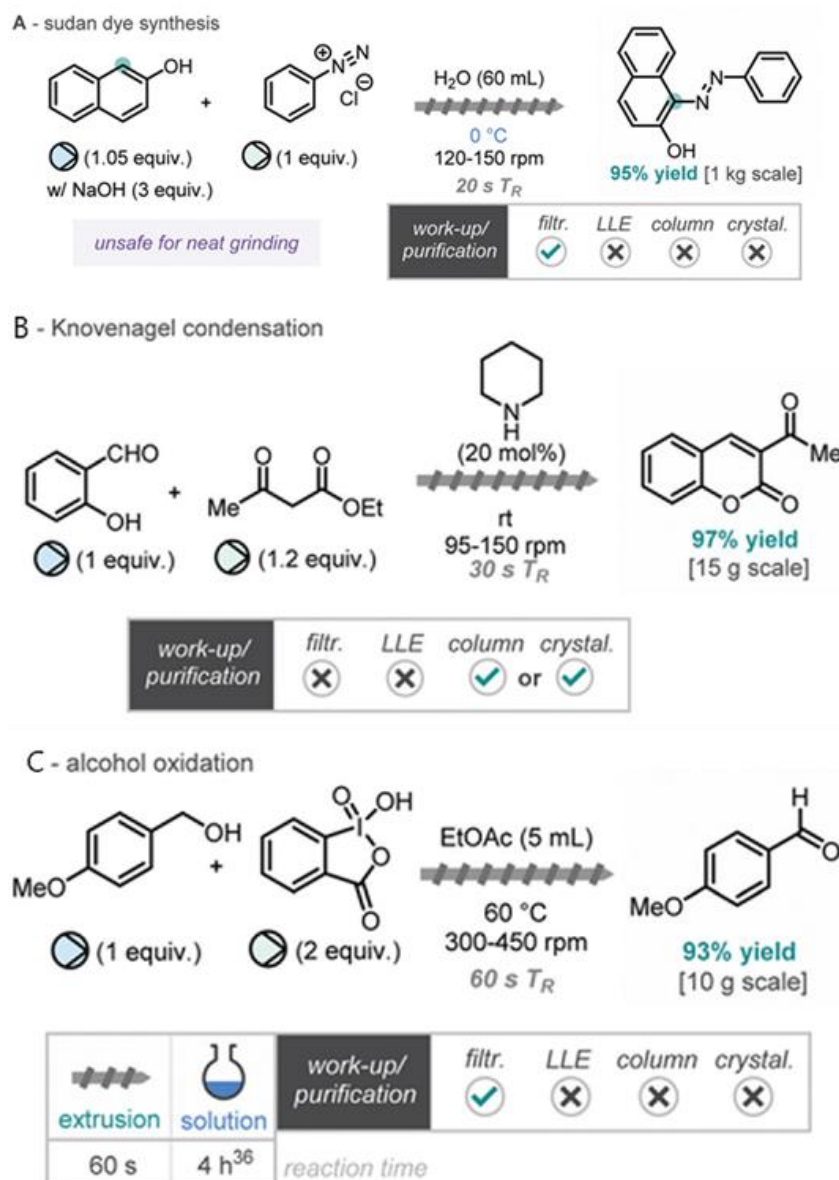


Figure 3: Several organic syntheses performed in the SSE setup [14]

2.1.2 Challenges

The reactions in Figure 3 are mainly solid-solid reactions. Liquid-liquid or liquid-solid reactions remain challenging because extrusion reactors often suffer from poor mixing efficiency when handling these reaction types. Achieving proper contact between reagents is crucial for higher reaction kinetics which is the case in solid-solid reactions. Bolt et al. report that solid-solid reactions for the synthesis of MOFs by reactive extrusion were most successful when the reactor temperature was above the melting point of the ligand [5]. Furthermore, reactions between liquids have not been studied by extrusion and may be more difficult to carry out. There are still very few examples of this reported in ball mill reactions. Secondly, reagents that are potentially explosive or that ignite when dry or exposed to friction are too

hazardous to be used in an extrusion process. For example, reactions using azides or hydrazones [12]. Additionally, the limited residence time and insufficient agitation reduce the mixing efficiency. Limited agitation favors mass transfer limitation which is the phenomenon when the chemical reaction cannot proceed at its intrinsic rate because the transfer of reactants or products to or from the reaction site is slower than the rate at which the reaction would occur if mass transfer limitations were absent. Mass transfer can exacerbate the formation of byproducts, reducing the yield of the desired product and complicating downstream processing [5], [15].

2.2 Macromixing and micromixing

Mixing reduces non-uniformities of several properties in the reactor, for example, temperature or viscosity [16]. Additionally mixing promotes mass transfer during chemical reactions. Product quality is dependent on the mixing conditions. The formation of by-products is known to be more prevalent when mixing is inefficient. The effect of mixing on a chemical reaction is dependent on the difference between reaction time t_r and mixing time t_m . If the mixing time is significantly shorter than the reaction time, then the reagents are well mixed before the reaction occurs. However, if the opposite is the case, then mass transfer limitation occurs which adversely affects product distribution and more by-products can form [17], [18]. Table 1 summarizes the three possible regimes based on the relative values of reaction time and mixing time.

Table 1: Summary of different regimes based on the relative value of t_m and t_r [19]

| Relative value of t_m and t_r | Regime | Description |
|-----------------------------------|---------------|--|
| $t_m \ll t_r$ | Slow | <ul style="list-style-type: none"> • Fast homogenization • Reaction rate limiting • Product distribution is chemically controlled |
| $t_m \approx t_r$ | Fast | <ul style="list-style-type: none"> • Product distribution Is controlled by both kinetics and mixing. |
| $t_m \gg t_r$ | Instantaneous | <ul style="list-style-type: none"> • Mass tranfer limiting • Product distribution is controlled by the degree of mixing |

The well-known mixing in food preparation, for example, is mixing on a macroscopic level i.e. macromixing. Therefore, macromixing can be described as the equal distribution of molecules throughout the reactor. In addition, there is micromixing which is mixing at the molecular level. The deformation of fluid elements characterizes this micromixing but also includes diffusion. As a result, micromixing enables distant molecules to more easily react over time. It is an important consideration in reactions where the reaction time is infinitesimally small compared to the mixing time or in reactions where the mixing time is comparable to the reaction time [20]. To study only micromixing effects, the rotation speed of the mixer and injection flow rate have to be adjusted to eliminate mass transfer limitations thereby facilitating optimal or efficient macromixing.

Figure 4 shows the difference between efficient and inefficient micromixing and efficient and inefficient macromixing. The colors relate to the color of reactor contents when using the Villermaux-Dushman method to study micromixing. Quadrants A and B are mixing outcomes in which macromixing is not limiting. Therefore, the difference in color of the solution is due to differences in micromixing efficiency. A more intense colored solution corresponds to more by-product formation hence inefficient micromixing. If macromixing is inefficient then micromixing is always inefficient. However, the converse is not always true and is dependent on the process parameters mentioned earlier. Quadrant C corresponds to the case in which macromixing is limiting hence local overconcentration can form in the reactor and provide competitive power to by-product formation.


| | | | |
|--------------------|--------------------|--------------------|---|
| | | Macromixing | |
| | | <i>Efficient</i> | <i>Inefficient</i> |
| Micromixing | <i>Efficient</i> | A | Not possible |
| | <i>Inefficient</i> | B |  C |

Figure 4: Different combinations macromixing and micromixing regimes

2.3 Experimental determination of micromixing efficiency

2.3.1 Methods of studying micromixing efficiency

Commonly, micromixing efficiency is studied by exploiting a pair of competitive reactions. Depending on the process conditions the degree of micromixing will differ. Colorimetric methods are also described in the literature. Table 2 shows a summary of different competitive reaction pairs that have been described in the literature. Additionally, alternative ways to determine micromixing efficiency exist. Those methods rely, for example, on the monitoring of a fluorescent dye or a pH-sensitive dye. An extensive list of methods is supplied by [21]. This thesis will investigate only the Villiermaux-Dushman method.

Table 2: Different options for studying micromixing

| Method | References |
|---|------------------------------|
| <i>Colorimetric</i> | |
| Formation of iron(III) cyanide complex | [22], [23], [24] |
| Hydrolysis of dichloroacetyl phenol red by sodium hydroxide | [25] |
| <i>Competing reactions</i> | |
| Villiermaux-Dushman reaction | [21], [26], [27], [28], [29] |
| 1-naphtol and 2-naphtol with diazotized sulfanilic acid | [30] |
| Bromination of 1,3,5-trimethoxybenzene | [31] |
| Bechamp reaction | [32] |

2.3.2 The Villiermaux-Dushman method

2.3.2.1 Principle

The Villiermaux-Dushman method is prevalently used to study micromixing in both batch and flow reactors for aqueous chemical systems. The method is based on the following pair of competitive reactions (reactions 1 and 2):



Reaction 1 is the protonation reaction of boric acid (H_3BO_3) and proceeds nearly instantaneously. Reaction 2 is the synproportionation reaction of iodine i.e. a redox reaction in which the same chemical species is being reduced and oxidized at the same time. By adding an excess amount of iodide (I^-), the formed iodine (I_2) will react with the excess amount of iodide ions in the solution and form triiodide ions (I_3^-) via reaction 3. Reaction 2 is considered fast but still slower than reactions 1 and 3 [21], [26], [28].



In the case of efficient micromixing, the injected hydrogen ions (H^+) are mainly consumed by reaction 1. As a result, the second and by extension, the third reaction will not proceed as much, and less triiodide is formed. This results in a less intense colored solution. In the case of inefficient micromixing, local over-concentrations of hydrogen ions are created in the solution which will change the competition between the reactions stated earlier. Inefficient mixing causes the second reaction to gain competitive power over reaction 1 because the stoichiometric ratio of reactants has become more favorable to the formation of iodine and subsequently triiodide. Therefore, the concentration of triiodide in a solution after mixing is a measure of micromixing quality provided that macromixing limitations are non-existent. The Villermaux-Dushman method uses UV-spectroscopy and the application of the Lambert-Beer law to measure the concentration of formed triiodide in the reaction medium [21], [26], [28].

2.3.2.2 Single injection method and Multiple injection method

A single injection method is often used to study micromixing. The injection volume of acid should be chosen carefully and poses no problem as long as the measured response is linear. Additionally, the injected amount of acid should also be large enough such that the change in optical density is measurable. For large reactors ($V \geq 1$ l), the amount of reagents needed is significantly greater therefore a multiple injection method is more beneficial. Following this method, one batch would provide more data points [26].

2.3.2.3 Quantification of micromixing quality

Guichardon characterized the micromixing quantitatively by introducing the term ‘segregation index’ X_s whose value lies between 0 and 1. A value of 0 corresponds to perfect micromixing while a value of 1 corresponds to perfect segregation. The formulas described below are usable for the single injection method. Equation 1 shows the relation between segregation index X_s and quantities Y and Y_{ST} . The latter two quantities are a function of the concentration of different reagents used c_i , the reactor volume $V_{reactor}$, and injection volume $V_{injection}$. Equation 2 shows that parameter Y is the ratio of the number of moles of acid consumed by reaction 2 to the total amount of moles of acid that was added. Equation 3 shows that Y_{ST} is the value of Y in the case of total segregation i.e. when micromixing proceeds infinitely slow [26].

$$X_s = \frac{Y}{Y_{ST}} \quad (\text{Equation 1})$$

$$Y = \frac{2 \cdot V_{reactor} \cdot (C_{I_2} + C_{I_3^-})}{V_{injection} \cdot C_{H^+}} \quad (\text{Equation 2})$$

$$Y_{ST} = \frac{\frac{c_{IO_3^-}}{[6 \cdot \frac{c_{H_3BO_3}}{c_{IO_3^-}}]}}{\frac{c_{IO_3^-}}{[6 \cdot \frac{c_{H_3BO_3}}{c_{IO_3^-}}] + 1}} \quad (\text{Equation 3})$$

The term C_{I_2} is an unknown and is not directly measurable with the Villermaux-Dushman method. However, by using the following system of equations the concentration of iodine can be calculated. Equation 4 is the mass balance for iodine. Equation 5 relates the concentrations of the different iodine species to the equilibrium constant K_B . Equation 6 shows that the equilibrium constant K_B is a function of temperature [33].

$$C_I^- = (C_I^-)_0 - \frac{5}{3}(C_{I_2} + C_{I_3^-}) - C_{I_3^-} \quad (\text{Equation 4})$$

$$K_B = \frac{C_{I_3^-}}{C_{I_2} \cdot C_I^-} \quad (\text{Equation 5})$$

$$\log_{10} K_B = \frac{555}{T} + 7.355 - 2.575 \cdot \log_{10} T \quad (\text{Equation 6})$$

Villermaux described another quantity related to segregation index X_S namely the micromixedness ratio α . Equation 7 shows the relation between segregation index X_S and micromixedness α . A high value of α corresponds to a low value of X_S hence better micromixing quality [34].

$$\alpha = \frac{1-X_S}{X_S} \quad (\text{Equation 7})$$

An important aspect of the multiple injection method is the slightly different calculations to acquire segregation indexes for each data point. After each injection, the initial concentrations of the compounds inside the reactor have to be recalculated. Equations 8 – 12 show the formulas needed for the calculations. Equations 8 -10 can be used to calculate the concentrations of IO_3^- , $H_2BO_3^-$, and I^- at the start of the i th injection. The quantities $\Delta n(I_2)_i$ and $\Delta n(I_3^-)_i$ and the amount of moles of iodine and triiodide formed exclusively during injection i which can be solved indirectly from equation 11 and the calibration line respectively. Equation 12 represents the ratio of the amount of acid consumed by reaction 2 to the amount of acid injected. Equation 13 shows the same ratio but in the case of total segregation. In this case, reactions 1 and 2 proceed significantly faster than mixing. Injected acid is consumed in proportion to borate and iodate ion concentrations. Equation 14 is used to calculate the segregation index after injection i .

$$C(IO_3^-)_{0,i} = \frac{C(IO_3^-)_{0,i-1}V_{reactor,i-1} - \frac{1}{3}[\Delta n(I_2)_i + \Delta n(I_3^-)_i]}{V_{reactor,i-1}} \quad (\text{Equation 8})$$

$$C(H_2BO_3^-)_{0,i} = \frac{C(H_2BO_3^-)_{0,i-1}V_{reactor,i-1} - [n_{H^+,injected} - 2*(\Delta n(I_2)_i + \Delta n(I_3^-)_i)]}{V_{reactor,i-1}} \quad (\text{Equation 9})$$

$$C(I^-)_{0,i} = \frac{C(I^-)_{0,i-1}V_{reactor,i-1} - \left[\frac{5}{3}(\Delta n(I_2)_i + \Delta n(I_3^-)_i) - \Delta n(I_3^-)_i\right]}{V_{reactor,i-1}} \quad (\text{Equation 10})$$

$$\frac{-5}{3}[C(I_2)_i]^2 + \left(C(I^-)_{0,i} - \frac{8}{3}C(I_3^-)\right) * [C(I_2)_i] - \frac{C(I_3^-)_i}{K_B} = 0 \quad (\text{Equation 11})$$

$$Y_i = \frac{2*[\Delta n(I_2)_i + \Delta n(I_3^-)_i]}{n_{H^+,inj}} \quad (\text{Equation 12})$$

$$Y_{ST,i} = \frac{6C(IO_3^-)_{0,i}}{6C(IO_3^-)_{0,i} + C(H_2BO_3^-)_{0,i}} \quad (\text{Equation 13})$$

$$X_{S,i} = \frac{Y_i}{Y_{ST,i}} \quad (\text{Equation 14})$$

2.4 Villermaux-Dushman method used in batch experiments

2.4.1 Determination of the chemical system

Before studying micromixing in batch, the chemical system has to be established. Typically for batch experiments, two solutions are used, namely a buffer solution and a sulfuric acid solution. Table 3 shows the composition of the buffer solution as proposed by different sources.

Table 3: Buffer composition for aqueous solutions (Volume = 5 l) [21], [26], [27], [35]

| Compound | Chemical formula | Concentration (mol/l) |
|------------------|------------------|-----------------------|
| Boric acid | H_3BO_3 | 0.1818 |
| Sodium hydroxide | NaOH | 0.0909 |
| Potassium iodate | KIO_3 | 0.0117 |
| Potassium iodide | KI | 0.0023 |

This buffer keeps the pH at around 9.15. The pH should be kept at a value greater than 7 to prevent premature formation of triiodide, but also as close as possible to 7 because at pH values greater than 10, the formation of hypoiodite ions is facilitated through reactions 4 and 5 [27].



2.4.2 Effect of the reactor dimensions

To effectively study micromixing efficiency, the effect of macromixing has to be perfected inside the reactor. For example, by introducing baffles which eliminate to formation of dead zones within the reactor. In addition, a round-bottom batch reactor can be used while also considering the ratio of reactor diameter to impeller diameter. Furthermore, at high rotational speeds, centrifugal forces on the liquid can create vortices in unbaffled reactors. This changes the mixing pattern and thus affects the mixing in batch reactors [32]. Different batch reactors with different measurements are described in the literature however the segregation indexes that are determined by these different studies are not comparable because segregation indexes are dependent on the concentrations of the used reagents and triiodide formed in the process. Therefore, a quantity that is concentration-independent was introduced namely micromixing time (t_{micro}) [35]. The micromixing time is the time needed to completely mix the system on a molecular scale. Alternatively, it can be defined as the time required for the reagents to diffuse to one another. The mixing efficiency controls the selectivity, quality, and distribution of the final product provided that the micromixing time, t_{micro} , is greater than the reaction time, t_{react} [19].

2.4.3 Effect of injection time on micromixing efficiency

Figure 5 shows the influence of injection time on the segregation index X_s i.e. micromixing efficiency. The influence of injection time on micromixing efficiency follows a decreasing exponential reaching a plateau phase after a critical injection time t_{crit} beyond which the macromixing time is much smaller than the injection time and only micromixing can be studied [18]. On the other hand, a rapid acid injection hence a high injection flow rate results in the creation of H^+ over-concentrated regions within the reactor which corresponds to increased triiodide formation and therefore a lower micromixing efficiency and higher segregation index.

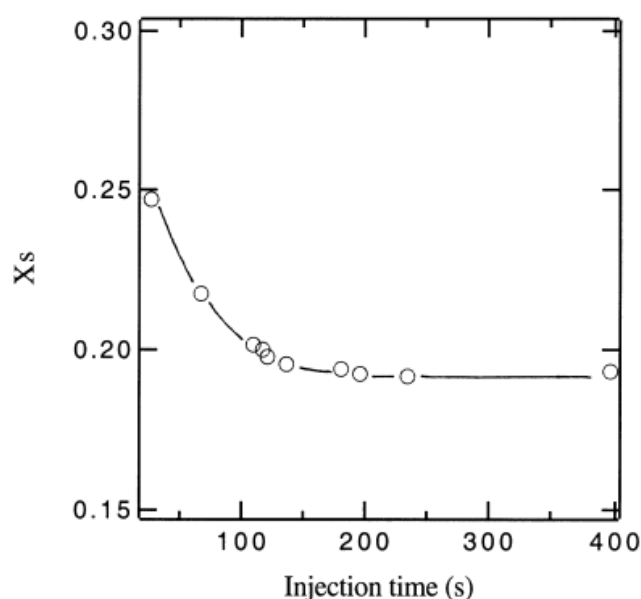


Figure 5: Influence of injection time on micromixing efficiency [26]

Guichardon performed a multiple injection method in which the process parameters i.e. the injection flow rate and rotation speed of the mixer were kept constant [26], [36], [37]. Therefore, segregation indexes and micromixing efficiency are expected to remain constant. Figure 6 confirms this trend. The acquired data points are therefore duplicates of one another.

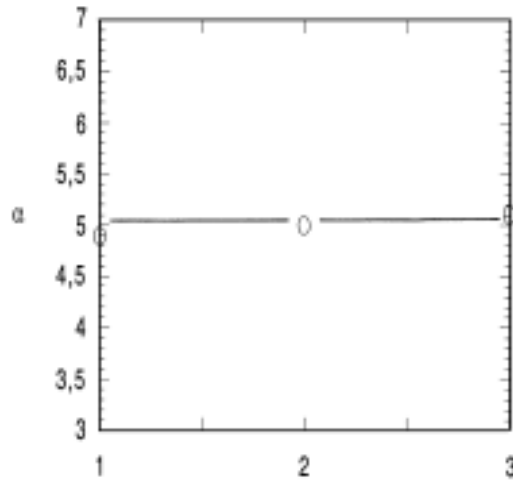


Figure 6: Segregation indexes between different injections inside the same batch reactor (Parameter α is the micromixedness factor which is proportional to the segregation index X_s) [26]

Another perspective of the multiple injection method is to vary either the stirring speed or the injection flow rate between different injections within the same batch. Therefore, segregation indexes and micromixing efficiency are not expected to remain constant but follow a similar decreasing exponential with increasing stirring speed following Figure 5. The acquired data points are not duplicates of one another. This perspective of multiple injections is powerful because more data can be gathered by using a minimal amount of reagents.

2.4.4 Effect of the rotation speed of the impeller on micromixing efficiency

Figure 7 shows the influence rotational speed on the segregation index X_s for different flow rates marked by numbers 1 to 5 from high to low flow rate. A higher stirring speed makes it less evident for H^+ overconcentrated regions to form, hence less triiodide is formed and micromixing is more efficient. Figure 7 implies that there is a critical stirring speed ω_{crit} beyond which the segregation index reaches a plateau phase. Furthermore, the differences in segregation index for different flow rates at a fixed stirring speed are more pronounced at low stirring speeds. This is evident because, at higher stirring speeds, the macromixing time has become sufficiently small such that the only differences in segregation index are due to micromixing effects only [38].

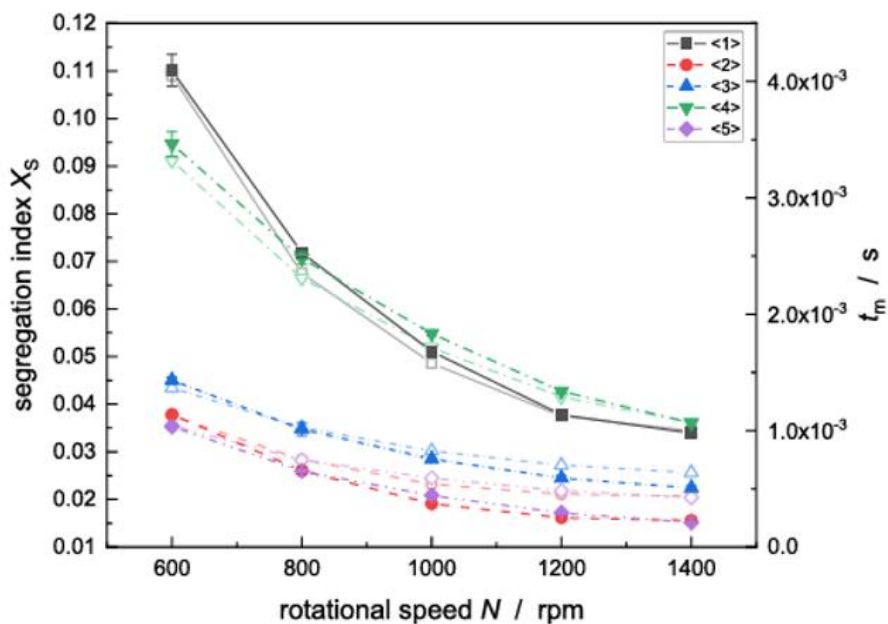


Figure 7: Effect of stirring speed on micromixing efficiency with $\omega_{crit} = 1200$ rpm [38]

2.4.5 Effect of backmixing in tubing on micromixing efficiency

Figure 7 shows the micromixing efficiency as a function of injection time at different rotational speeds of the mixer. When the injection time and stirring speed are high, the bulk reactants are pushed back into the feed pipe which causes pre-reaction in the tubing under poor mixing conditions. Pipe diameter also plays a role in potential back mixing. Figure 8 shows that a larger pipe diameter exacerbates back mixing. Assirelli et al. attribute this to the decreasing exit velocity of the feed pipe [39].

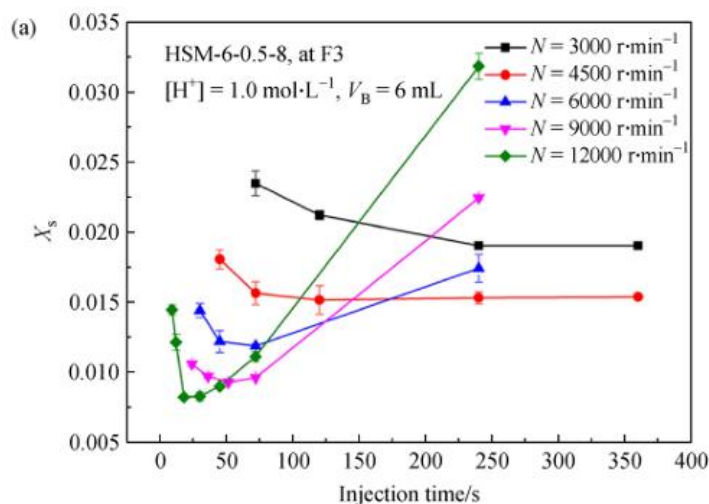


Figure 8: Effect of back mixing of micromixing efficiency [40]

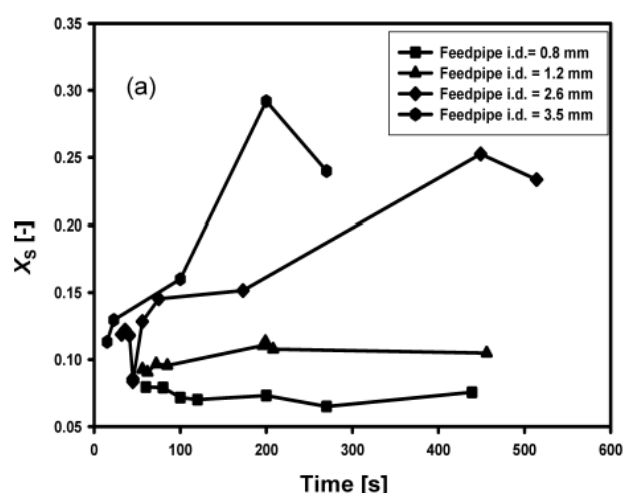


Figure 9: Effect of pipe internal diameter on back mixing and micromixing efficiency [39]

2.4.6 Mixing experiments in viscous media

Due to the increasing interest in solvent-free process intensification, the Villermaux-Dushman method should be upscaled for use in mixing experiments in higher-viscosity solutions. Guichardon investigated the micromixing process for viscosities up to 170 mPa·s by the addition of glycerine. Glycerine causes the initial boric acid buffer to change color from colorless to yellow-orange prematurely. This is not due to the acidity of glycerin ($K = 7 \cdot 10^{-15}$) nor by oxidation of glycerin by reactants inside the buffer solution. Glycerin does cause the redox potential of the iodine/water couple to shift thereby promoting premature iodine formation which corresponds to discoloration [41]. Reaction 6 shows that increasing the pH from 9.15 to 11.00 favors iodine disproportionation and the yellow-colored buffer turns colorless. The buffering region of the borate buffer shifts from $\text{pH} = 9.15 \pm 1$ to $\text{pH} = 11.00 \pm 1$. Figure 9 shows that the influence of injection time on micromixing experiments is similar to aqueous solutions.



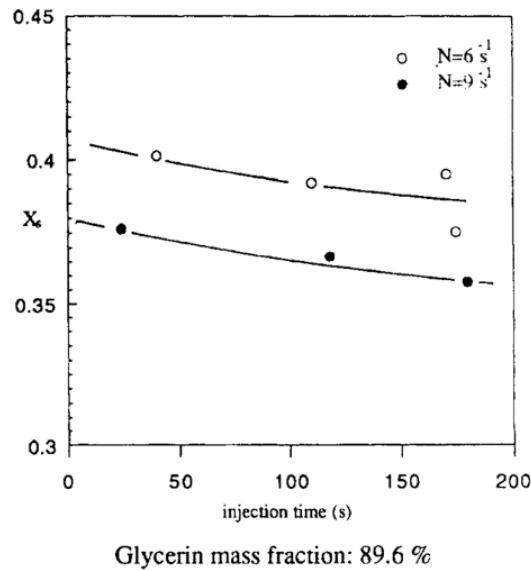


Figure 10: Effect of injection time of micromixing efficiency in viscous medium of 170 mPa·s. The data points were received through mixing experiments in a 1 l stirred tank reactor [41]

Other viscosifying agents are described throughout literature. Arian and Pauer have used sucrose in their mixing experiments to vary the viscosity up to 6 Pa·s. Sucrose is a promising candidate to use when preparing buffer solution with viscosities greater than 0.2 Pa·s. However, some caution is needed due to possible acid-catalyzed cleavage of sucrose. The cleavage of sucrose corresponds to glucose formation which can react with iodine and will perturbate results [28]. Pinot et al. have used hydroxyethylcellulose (HEC) to vary the viscosity from 1 mPa·s to 50 mPa·s which corresponds to 0 wt% HEC and 0,5 wt% respectively. The influence of injection time on micromixing was similar to aqueous solution and glycerine-water solutions [27]. Figure 11 shows the influence of stirring speeds N on the micromixedness ratio α for different concentrations of HEC hence different viscosities. Increasing the viscosity causes α to decrease and following Equation 7, the segregation index rises. Therefore, the micromixing efficiency decreases as well.

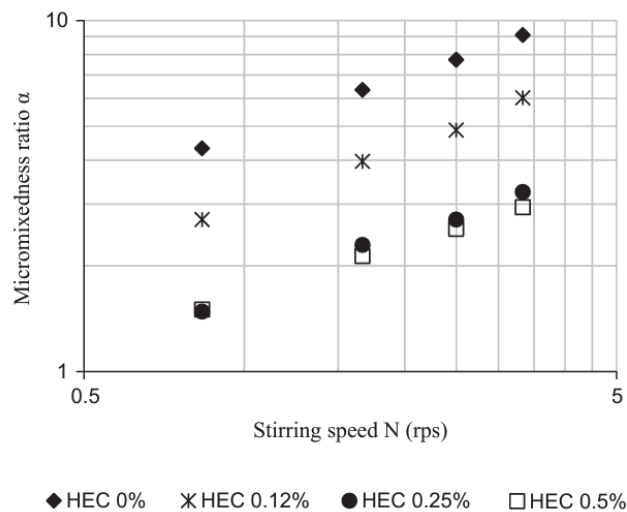


Figure 11: The influence of stirring speeds N on the micromixedness ratio α for different concentrations of HEC hence different viscosities [27]

The Kolmogorov length scale η (Equation 16) shows that a smaller viscosity gives rise to smaller turbulent eddies which can quickly homogenize the solution by distributing reactants uniformly and hamper the accumulation of H^+ excess regions in the reactor. Therefore, micromixing is expected to be

more efficient in aqueous solution. Parameter ν is the viscosity of the mixture and ε is the energy dissipation rate [44].

$$\eta = \left(\frac{\nu^3}{\varepsilon}\right)^{0.25} \quad (\text{Equation 16})$$

2.5 Villiermaux-Dushman method used in flow experiments

The Villiermaux-Dushman method has been applied to flow reactors of which there are many variants. Examples are gas-liquid vortex reactors [42], milli-flow reactors [35], and microflow reactors [35]. Although Gobert et al. studied milli flow tubular reactors which are at a smaller scale than reactive extrusion, the results can be useful because an extrusion reactor is in a way a tubular reactor. An increase in Reynolds number decreases the micromixing time which is evident because a higher Reynolds number corresponds to more engulfment and vortices formation. The calculation of Reynolds numbers in flow reactor can be calculated with Equation 17 in which ρ is the fluid density, D is reactor diameter, μ is the viscosity of the fluid and v is the linear velocity of the fluid. For $Re > 3500$, the flow is in turbulent regime and mixing is promoted while for $Re < 2300$, the flow regime is laminar.

$$Re = \frac{\rho v D}{\mu} \quad (\text{Equation 17})$$

The effect of reactor length on micromixing efficiency was studied which showed that only the first meter of the used reactor with an internal diameter 0.4 mm and length 12 m had a significant influence on the segregation index. This implies that if the micromixing times are sufficiently short such that a certain reaction becomes kinetically controlled then it is beneficial to reduce the reactor size. However, this is only true for reaction with similar kinetics as the Villiermaux-Dushman reactions. [35].

Furthermore, the calculation of the segregation index in flow experiments is simpler than in batch experiments because fresh reagents are supplied continuously which is not the case in batch. Equations 18 – 20 are used to calculate the segregation index which are similar to equations 12-14 however volumes V are replaced by flow rates Q [35].

$$Y = 2 \left(\frac{C_{I_3^-} * Q_{I_3^-}}{C_{H_0^+} * Q_{H_0^+}} \right) \quad (\text{Equation 18})$$

$$Y_{ST} = \frac{6C(I O_3^-)_0}{6C(I O_3^-)_0 + C(H_2 B O_3^-)_0} \quad (\text{Equation 19})$$

$$X_s = \left(\frac{Y}{Y_{ST}} \right) \quad (\text{Equation 20})$$

3 Materials and Methods

3.1 Triiodide quantification

3.1.1 Villiermaux-Dushmann method: Triiodide formation

The Villiermaux-Dushmann method was employed for the quantification of triiodide. The chemical system consists of two competitive parallel reactions in which the amount of triiodide formed is a measure of mixing efficiency. Reactions 7-9 show that the formation of iodine requires local overconcentration of H^+ whereas the formation of boric acid does not. During this method, a large excess of iodide is needed to facilitate the triiodide formation.



3.1.2 Analytical method: UV-VIS spectroscopy

Triiodide has been reported to absorb light of wavelength 353 nm. Therefore, UV-VIS spectroscopy was chosen as the analytical method. Using a (Thermo Scientific - Genesys 10S) spectrophotometer the absorption spectrum of triiodide was determined to confirm 353 nm as a viable wavelength but also to investigate if other wavelengths are usable, for example, if absorbance measurements at 353 nm lay outside the linear range. Four wavelengths were considered for the analyses namely 353 nm, 410 nm, 450 nm, and 476 nm. The linear ranges for these four wavelengths were determined for both aqueous solutions and solutions with a viscosity of 100 mPa·s. For this, a 100 ml stock solution of triiodide (10 mM) was made. Subsequent dilutions up to a factor of 300 were made with ultra-pure water. Table 4 shows the composition of the stock solution for both 1 mPa·s and 100 mPa·s. Glycerol was used as a viscosifying agent. The used compounds were dissolved in sulphuric acid solution (0.03 M) for the stock solution preparation.

Table 4: Composition of the stock solution (100 ml)

| Compound | CAS-nr | Manufacturer | Aqueous stock solution (1 mPa·s) | Viscous stock solution (100 mPa·s) |
|--|-----------|---------------|----------------------------------|------------------------------------|
| Potassium iodide (KI) | 7681-11-0 | Sigma-Aldrich | 0.0117 M | 0.0117 M |
| Potassium iodate (KIO ₃) | 7758-05-6 | Sigma-Aldrich | 0.0023 M | 0.0023 M |
| Glycerol (C ₃ H ₈ O ₃) | 56-81-5 | | - | 0.945 M |
| Sulphuric acid (H ₂ SO ₄) | 7664-93-9 | VWR | 0.03 M | 0.03 M |

3.2 Mixing experiments

3.2.1 Preparation of solutions

Two solutions were prepared specifically a sulphuric acid solution (0.36 M) and a buffer solution with However, it did not contain sulphuric acid because this would result in the premature formation of triiodide which makes mixing experiments obsolete. Ultra-pure water was used to dissolve the components. The order of dissolution of components was important. First, boric acid and sodium hydroxide were dissolved in water to establish a buffered solution of pH 9.15. Second, potassium iodide and potassium iodate were dissolved in the buffered solution and water was added to reach the required total volume. For a viscous solution, an appropriate amount of water was substituted by glycerol. Table 5 shows the composition of buffer solutions used.

Table 5: Composition of acid and buffer solution for mixing experiments

| Compound | CAS-nr | Manufacturer | Aqueous stock solution (1 mPa·s) | Viscous stock solution (100 mPa·s) |
|--|------------|---------------|----------------------------------|------------------------------------|
| Boric acid (H ₃ BO ₃) | 10043-35-3 | VWR | 0.1818 M | 0.1818 M |
| Sodium hydroxide (NaOH) | 1310-73-2 | VWR | 0.0909 M | 0.1818 M |
| Potassium iodide (KI) | 7681-11-0 | Sigma-Aldrich | 0.0117 M | 0.0117 M |
| Potassium iodate (KIO ₃) | 7758-05-6 | Sigma-Aldrich | 0.0023 M | 0.0023 M |
| Glycerol (C ₃ H ₈ O ₃) | 56-81-5 | VWR | - | 0.945 M |
| | | | | |
| Sulphuric acid (H ₂ SO ₄) | 7664-93-9 | VWR | 0.36 M | 0.36 M |

3.2.2 Batch experiments

First, the buffer solution was loaded in an OptiMax reactor vessel (1000 ml). Next, the sulphuric acid solution was injected into the buffer solution using a pump (ISCO 260D Syringe Pump) to start the parallel competitive reactions 7 and 8. After the injection of the acid, samples were taken and analyzed. Figure 12 shows a schematic representation of the batch setup with solutions A (acid) and B (buffer). The used mixer was one integrated into the OptiMax reactor.

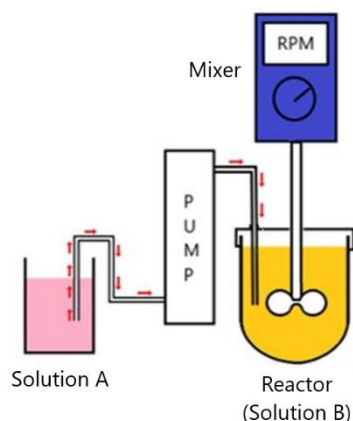


Figure 12: Batch setup

The considered parameters were injection volume, injection flow rate, and stirring speed of the mixer. Table 6 shows parameter ranges. A single injection method was barred due to the large reactor volume and amount of reagents needed. Therefore a multiple injection method was opted to minimize reagent use and gain more data per batch experiment.

Table 6: Parameter ranges (Batch)

| Parameter | Range |
|---|-------------------|
| Rotation speed (ω) | [100 - 700] rpm |
| Injection flow rate (Q) | [0.2 - 20] ml/min |
| Injection time (min) | [2 - 0.1] min |
| Viscosity of buffer solution (η) | [1 - 100] mPa·s |
| Injection volume (V_{inj}) | [0.4 - 2] ml |

Guichardon performed experiments in a batch reactor similar to the OptiMax reactor vessel (1000 ml) in which the injection volume was 2 ml and the concentration of H⁺ was 1 mol/l. Only three to four injections per batch were possible this way. Therefore, to increase the amount of possible injections per batch, the concentration of acid was lowered to 0.72 mol/l. This way five injections were possible per batch and a complete sweep of stirring speeds was possible. The injection volume was 2 ml for aqueous solutions and 1 ml for 100 mPa·s solutions.

Next, stirring speed sweeps were performed at different injection flow rates to determine the optimal injection flow rate at which only micromixing can be studied. During these experiments, the stirring speed was varied in between injections. The injection flow rate varied in between batches. Table 7 shows an experimental map in which every row corresponds to one batch experiment. Batch experiments were performed twice, therefore $n = 2$.

Table 7: Stirring speed sweeps at different injection flow rates

| Injection flow rate (ml/min) | Rotation speed (rpm) | | | | |
|------------------------------|----------------------|-----|-----|-----|-----|
| | 100 | 200 | 350 | 500 | 700 |
| 0.5 | | | | | |
| 1 | | | | | |
| 2 | | | | | |
| 10 | | | | | |
| 20 | | | | | |

3.2.3 Flow experiments

During flow experiments, buffer, and acid solutions were continuously injected into the single screw extrusion reactor (working volume = 20 ml) by using separate pumps (ISCO 500D Syringe Pump and ISCO 260D Syringe Pump respectively). From the reactor outlet, the mixture was led to the spectrophotometer (Thermo Scientific - Genesys 10S) equipped with a flow cell. The VisionLite 5 software was used to collect absorbance data continuously. Figure 13 shows the flow setup.

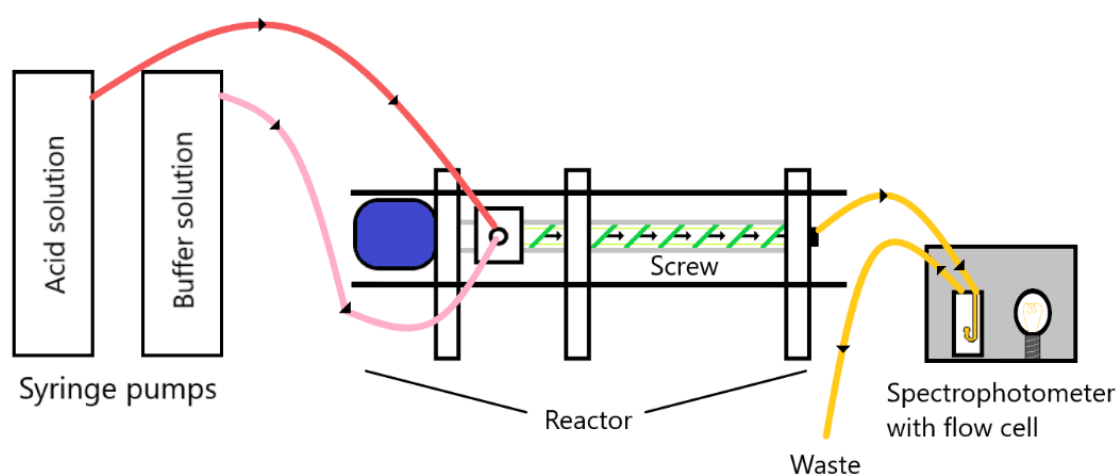


Figure 13: Flow experiment setup

The considered parameters were the stirring speed of the screw, the ratio of flow rates of buffer to acid R , mixing element type, and screw configuration. Table 8 shows the parameter ranges. The flow rate of the buffer solution was kept at 20 ml/min. Therefore, any changes of ratio R were due to changes in acid flow rate.

Table 8: Parameter ranges (flow)

| Parameter | Range |
|---|-----------------------|
| Stirring speed of screw (ω) | [100-400] rpm |
| Flow rate ratio (R) | [75-125] |
| Acid flow rate (q_{H^+}) | [0.160-0.267] ml/min |
| Viscosity of buffer solution (η) | [1 - 100] mPa·s |
| Mixing element type | [Normal pin – Saxton] |
| Screw configuration | [MTM; MTT; MTM*] |

First, experiments were done in aqueous solutions to establish an optimal ratio R such that at the lowest stirring speed, absorbance measurements were below the upper limit of the linear range. Table 9 gives an overview of these experiments. Both mixing elements were tested with a screw configuration MTM with M corresponding to a mixing element and T corresponding to a transport element.

Next, stirring speed sweeps were done at a ratio R of 125 for two mixing element types namely Normal pin mixer and Saxton mixer in both aqueous and 100 mPa·s solutions. The screw configuration for these experiments was M-T-M. Additionally, the screw configuration was altered to M-T-T and M-T-M* with M = Saxton mixer and M* = Normal pin mixer to investigate the influence of the number of mixing elements implemented into the screw. Table 10 shows an experimental map of the different experiments that were executed. The investigated screw stirring speeds were 100, 167, 250, 300, and 400 rpm. The stirring speed was altered after a plateau was reached for the absorbance measurement at the previously set value for the stirring speed. The different flow experiments were mostly performed once, therefore n = 1.

Lastly, experimental data is compared to simulations. These simulation were done in Ansys Computation Fluid Dynamics software by first delineating the reactor dimensions which serves as borders that the fluid cannot cross during the simulation. Next, the simulation was started after which the software will use validated models to predict the flow path in the screw reactor. The simulation were executed for both Normal pin and Saxton mixing elements and also for both 1 mPa·s and 100 mPa·s solutions. From the simulations, the turbulent kinetic energy which are a measure of eddies energy and size.

Table 9: Optimization of ratio R for flow experiments

| Parameter | Experiment 1 | Experiment 2 | Experiment 3 |
|---------------------------|--------------|--------------|--------------|
| Buffer flow rate (ml/min) | 20 | 20 | 20 |
| Acid flow rate (ml/min) | 0.160 | 0.200 | 0.267 |
| Ratio R | 125 | 100 | 75 |

Table 10: Stirring speed sweeps for flow experiments

| Parameter | Experiment 1 | Experiment 2 | Experiment 3 | Experiment 4 |
|---------------------|--------------|--------------|--------------|--------------------------------|
| Ratio R | 125 | 125 | 125 | 125 |
| Mixing element | Normal pin | Saxton | Saxton | Saxton (M) and Normal pin (M*) |
| Screw configuration | M-T-M | M-T-M | M-T-T | M-T-M* |
| Viscosity (mPa·s) | 1 | 1 | 1 | 1 |
| | | | | |
| Parameter | Experiment 5 | Experiment 6 | Experiment 7 | Experiment 8 |
| Ratio R | 125 | 125 | 125 | 125 |
| Mixing element | Normal pin | Saxton | Saxton | Saxton (M) and Normal pin (M*) |
| Screw configuration | M-T-M | M-T-M | M-T-T | M-T-M* |
| Viscosity (mPa·s) | 100 | 100 | 100 | 100 |

4 Results

4.1 Batch experiments in OptiMax reactor

Batch experiments are performed to serve as a benchmark for flow experiments. The goal is to characterize micromixing in a batch reactor but also to master the Villermaux-Dushman method using the protocol devised by Guichardon et.al. An OptiMax reactor of 1000 ml was chosen and a multiple injection method was used. To use each batch experiment to the fullest, the stirring speed was altered in between injections while the injection time was varied in between batches. From the data, the critical injection time is determined first to make sure that only micromixing effects are studied and therefore serves as a filter. These experiments were done for aqueous solutions and 100 mPa·s solutions.

4.1.1 Aqueous medium

4.1.1.1 Optimization of injection time

Figure 15 shows that the segregation index is higher at shorter injection times and decreases toward a plateau phase for a fixed stirring speed. At a short injection time, macromixing limitations are more prevalent which facilitates the accumulation of H^+ excess regions in the reactor and subsequent formation of triiodide by-product. Therefore, segregation indexes are higher than at longer injection times at which added H^+ is homogenized faster and more boric acid is formed compared to triiodide. For injection times at the plateau phase only micromixing effects can be studied. For the OptiMax reactor (Reactor volume of 1000 ml), the critical injection time was 2 minutes. Any injection time greater than or equal to 2 minutes is sufficient to study only micromixing effects in this reactor. Guichardon et.al have found similar results shown in Figure 5.

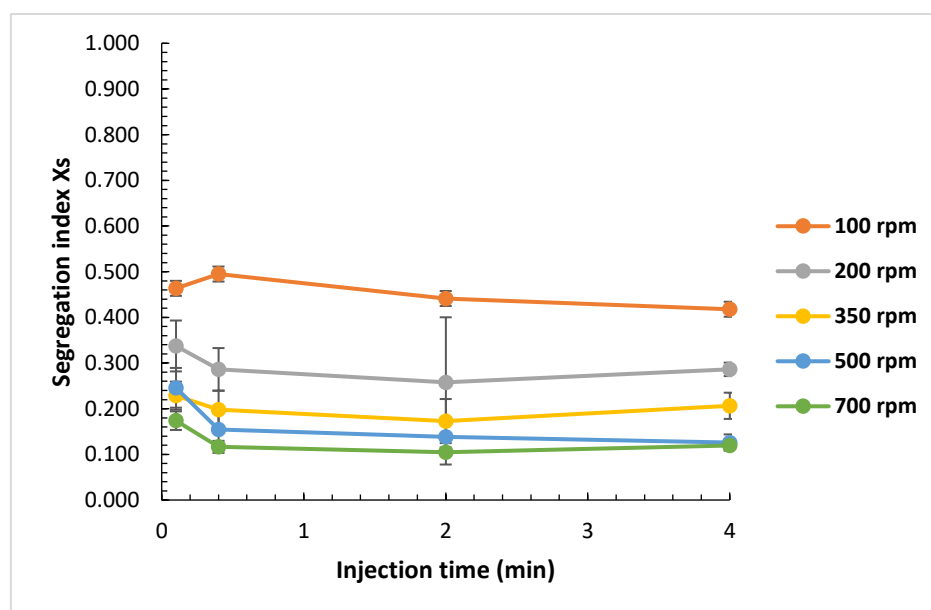


Figure 14: Optimization of injection time in OptiMax reactor for aqueous solutions (Injection volume = 2 ml and the concentration of acid = 0.36 M.. The investigated flow rates are 20 ml/min, 5 mL/min, 1 ml/min and 0.5 ml/min. Each data points was measure twice, $n = 2$. Each data point is an average segregation index value.)

4.1.1.2 Stirring speed sweeps

Figure 16 shows that the segregation index decreases as the stirring speed increases. At lower stirring speeds, the the accumulation of H^+ excess regions in the reactor is facilitated. Therefore, the segregation index is higher and the micromixing efficiency is lower. Increasing the stirring speed makes H^+ accumulation less possible, however a plateau is reached eventually because the process has become kinetically controlled. Both curves overlap because both injection times lie on the micromixing plateau. established in 4.1.1.1. While stirring speed sweeps were done at injection times smaller than the established critical injection time of 2 minutes, macromixing limitations dominate at these injection times. Therefore, the corresponding curves are not relevant to study micromixing effects and thus not shown in Figure 16

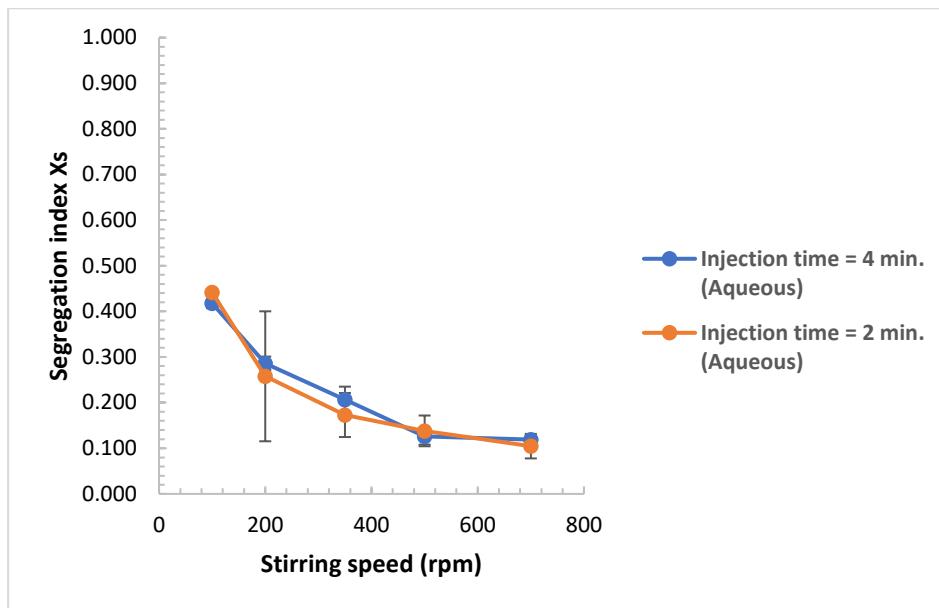


Figure 15: Stirring speeds sweep in OptiMax reactor for aqueous solutions. Each data point was measured twice, $n = 2$. Each point on the graph is an average segregation index value

4.1.2 Viscous medium $\eta = 100 \text{ mPa}\cdot\text{s}$

4.1.2.1 Optimization of buffer composition

Due to the premature yellow discolorization of the buffer solution when glycerol was added, the composition of the buffer was altered by adding extra sodium hydroxide. Figure 17 shows that the equivalence point and discoloration point coincide at a volume of 9 ml NaOH (1 mol/l). This amount should not be exceeded because this way an excess of hydroxide is introduced in the buffer which will react with the injected acid first hence a smaller amount of acid is left to react in the mixing experiment which distorts the results.

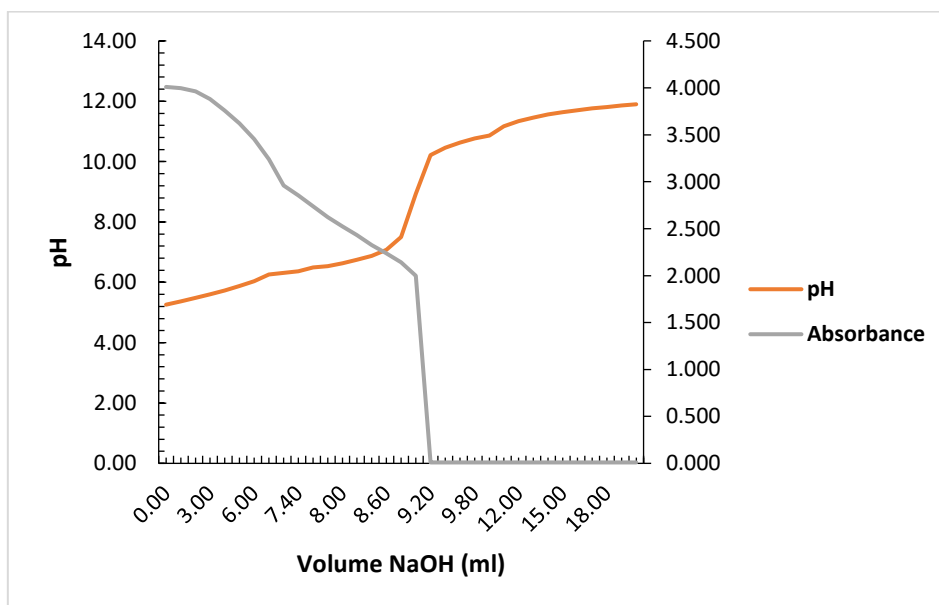


Figure 16: Titration curve of buffer solution with 83 m% glycerol (100 mPa·s). Titration was done with NaOH solution of 1 mol/l

4.1.2.2 Optimization of injection time

Figure 18 shows that the segregation index in viscous solution is higher than in aqueous solution. This difference can be attributed to differences in Kolmogorow length scale. The larger variations of the measurements can be attributed to improper sampling and the presence of bubbles. The relation between injection time and segregation index is similar to the relation in aqueous solution. For the OptiMax reactor (reactor volume = 1000 ml), the critical injection time is 1 minute. Therefore, injection times greater than or equal to 1 minute are sufficient to study micromixing effects only, when the viscosity of the mixture is 100 mPa·s and the injection volume is 1 ml.

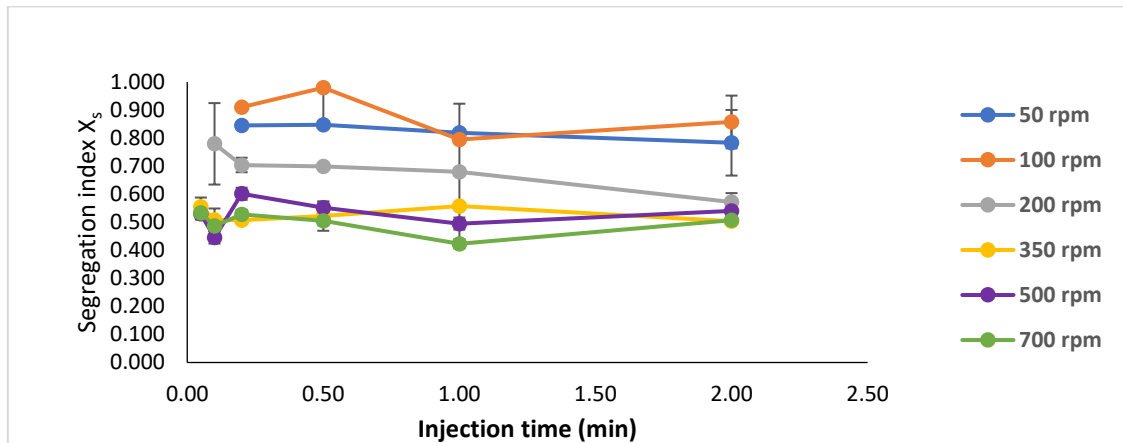


Figure 17: Optimization of injection time in OptiMax reactor (100 mPa·s). All data points were measured twice, $n = 2$

4.1.2.3 Stirring speed sweeps

In 100 mPa·s media, the stirring speed sweep shows that the segregation index follows a similar progression as the stirring speed increases. The same reasoning as 4.1.1.2. is applicable to explain these results. While stirring speed sweeps were done at injection times smaller than the established critical injection time of 1 minute, macromixing limitations dominate at these injection times. The corresponding curves are not relevant to study micromixing effects and thus not shown in Figure 19. The yellow curve corresponds to an injection time of 1 minute while the grey curve corresponds to an injection of 2 minutes. Both curves roughly overlap with each other because both injection times lie on the micromixing plateau.

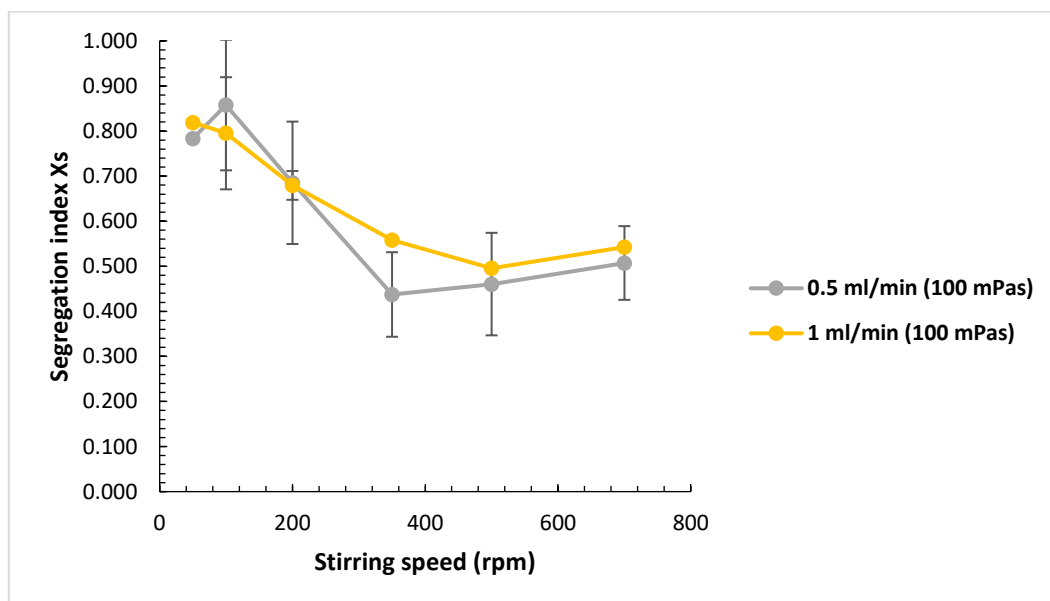


Figure 18: Stirring speed sweep in OptiMax reactor (100 mPa·s)

Figure 20 shows that micromixing is more efficient in aqueous media. More viscous solutions correspond to a lower Reynolds number where turbulence is minimal. Additionally, internal friction forces dissipate the kinetic energy added through mixing, which further minimizes turbulence. Turbulence is important to create eddies that enhance micromixing. Viscous solutions show more resistance to flow and deformation which complicates the generation and sustainment of eddies. The larger variations in the data points for 100 mPa·s solution can be attributed to improper sampling and/or air bubbles in the cuvet during measurement.

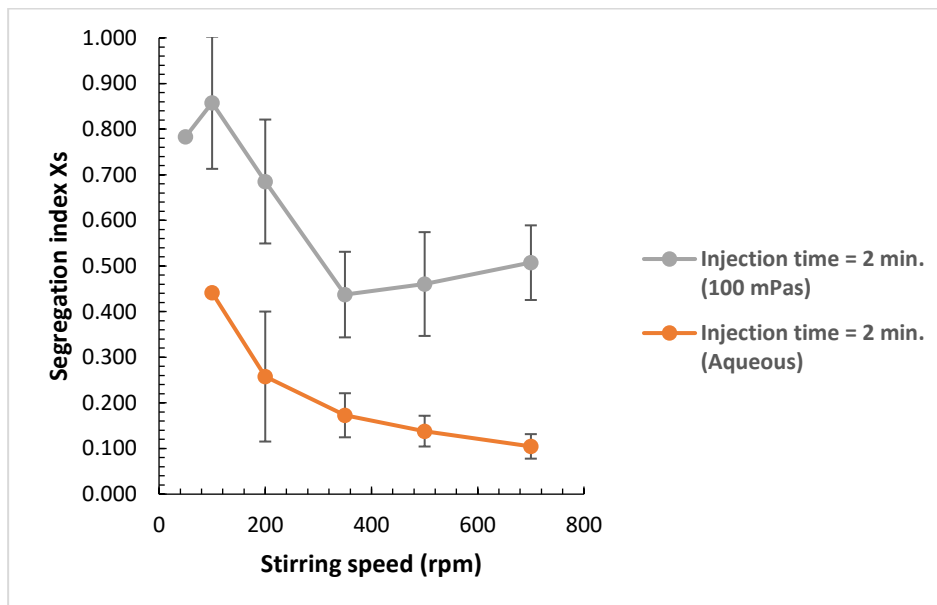


Figure 19: Micromixing efficiency in OptiMax reactor (Aqueous vs 100 mPa·s solution) if injection time is 2 minutes. All datapoints were measured twice, $n = 2$ Each point on the graph is an average segregation index value

4.1.3 Sub-conclusion

The batch experiments served as a benchmark to gauge if the Villermaux-Dushman method was viable in higher viscous systems. Critical injection times were determined and stirring speed sweeps were done for aqueous and 100 mPa·s solutions. The OptiMax reactor is therefore characterized within the used parameter ranges.

4.2 Flow experiments in Single-screw extrusion reactor

Flow experiments are performed to characterize micromixing in the screw reactor. The first objective is to investigate which mixing element enhances micromixing the most. A second objective is to investigate the influence of screw configuration on micromixing efficiency. Initial flow experiments are performed to find an optimal flow rate ratio R (Equation 21) by varying the acid flow rate while keeping the buffer flow rate constant at 20 ml/min.

$$R = \frac{Q_{buffer}}{Q_{acid}} \quad (\text{Equation 21})$$

Subsequently, two mixing elements specifically Saxton and Normal pin are studied in mixing experiments with screw configuration M-T-M. This is executed for both aqueous and 100 mPa·s solutions. Next, the influence of screw configuration on micromixing is studied in both aqueous and 100 mPa·s solutions.

4.2.1 Optimization of flow rate ratio R

Figure 21 shows that a flow rate ratio $R = 125$ is suitable for performing mixing experiments inside the reactor. Each absorbance measurement lies within the linear range and can therefore be translated into a segregation index X_s . For ratios 100 and 75, this was not the case. Therefore, further flow experiments in either aqueous or 100 mPa·s solution were done at a ratio $R = 125$.

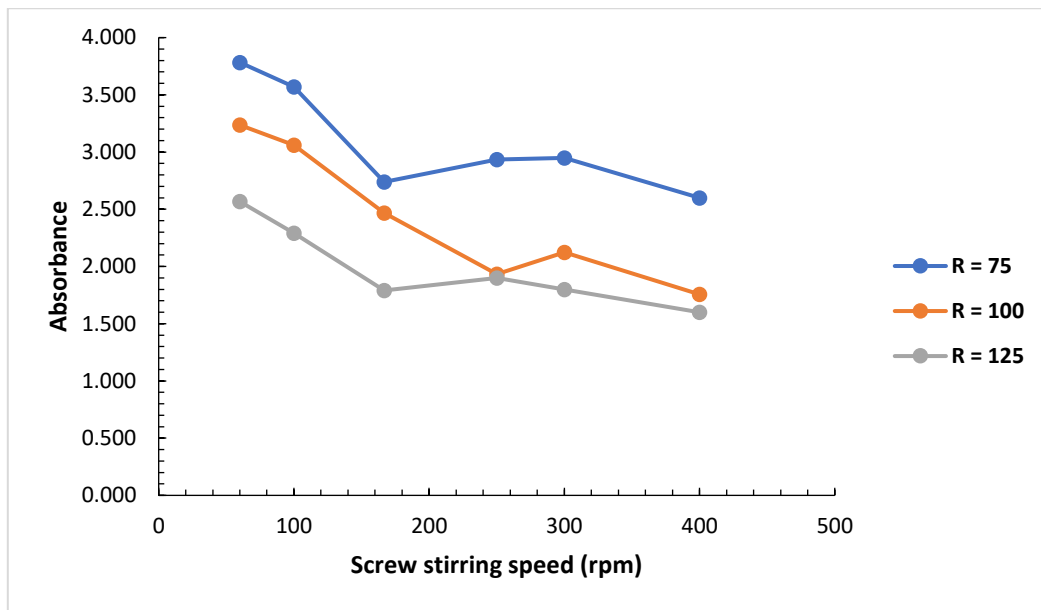


Figure 20: Optimization of flow rate R for normal pin mixer in aqueous solution. (Buffer flow rate was 20 ml/min while acid flow rate varied between 0.160 ml/min, 0.200 ml/min, and 0.267 ml/min which correspond to ratios 125, 100, and 75 respectively. Each data point was measured once, $n = 1$)

4.2.2 Variation of mixing element type

Figure 22 shows that Saxton mixing elements provide more optimal micromixing than Normal pin mixing elements in both aqueous and 100 mPa·s media. This can be explained by the differences in screw pattern geometry. The interrupted slotted flights of the Saxton mixing element enable fluid of different converging channels to mix as opposed to Normal pin mixing elements which do not have slotted flights. Furthermore, a greater micromixing efficiency is achieved in an aqueous solution independent of the used mixing element. This result can be explained through the Kolmogorov length scale η and shows that a smaller viscosity gives rise to smaller turbulent eddies which can quickly homogenize the solution by distributing reactants uniformly and hamper the accumulation of H^+ excess regions in the reactor [43]. The significant difference in segregation index at higher stirring speeds for the orange and blue curves can be attributed to measuring errors. These datapoints were measured once. Future repeat experiments will most likely resolve this error.

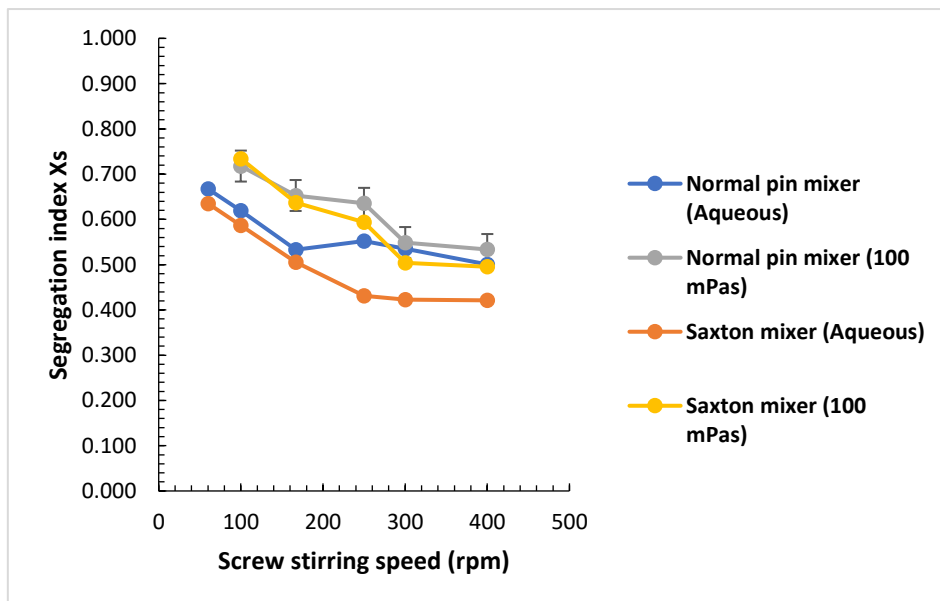


Figure 21: Effect of mixing elements types in aqueous and 100 mPa·s solutions for $R = 125$. All data point were measured once, $n = 1$ apart from the grey points which were measured twice, $n = 2$

These results were compared to Computational fluid dynamics (CFD) simulations. Figure 23 shows the acquired CFD-data. The average turbulent kinetic energy (TKE) is a measure of the intensity of turbulence in a fluid. Alternatively, it can be defined as the amount of energy available to create and sustain eddies. TKE is related to the turbulent Reynolds number Re_T through Equation 22 and is defined as the ratio of inertial forces to viscous forces within the turbulent eddies. This is different from the normal Reynolds number which is defined as a similar ratio but within the flow as a whole [44].

$$Re_T = \frac{\sqrt{(TKE)*l}}{\mu} \quad (\text{Equation 22})$$

A higher TKE means that turbulence inside the fluid is more vigorous which leads to smaller and more energetic eddies. The simulations show that the TKE is higher for aqueous solutions compared to 100 mPa·s solutions and higher for Saxton mixing elements compared to Normal pin mixing elements. This is because Saxton mixing elements have interrupted slotted flights that enables fluid from neighboring channels to mix in comparison to Normal pin mixing elements which do not have interrupted slotted flights. Additionally, Figure 23 shows a large difference in average turbulent kinetic energy for aqueous and 100 mPa·s solutions although the difference in segregation index significantly smaller between both viscosities. Micromixing is not only dependent on segregation index but also of molecular diffusion and kinetics which most likely do not scale linearly with the average turbulent kinetic energy.

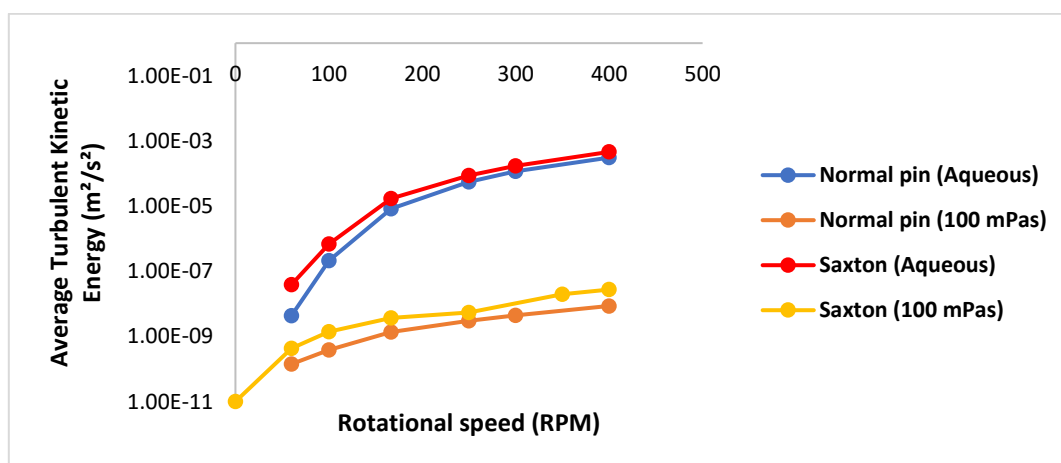


Figure 22: CFD simulations for mixing in screw reactor

4.2.3 Variation of screw configuration

Figure 24 shows that screw configuration, which is the sequence of installed screw elements, has no significant effect on micromixing efficiency for both aqueous and 100 mPa·s media. Implementing a mixing element right before the reactor outlet does not further enhance micromixing. The parallel competitive reactions are considered significantly fast which implies that the reaction is complete after mixing by the first mixing element that the fluid encounters. A similar result was obtained by Gobert et al [35]. The configuration T-M-T was deemed obsolete because a difference in micromixing efficiency was observed between Saxton and Normal pin mixing element for the configuration M-T-M. Therefore, it is unlikely that the reaction has gone to completion before it reaches the first mixing element of the screw. The screw stirring speed has a greater influence on micromixing efficiency than screw configuration because it has a direct impact on the accumulation of H^+ excess regions. An increase in stirring speed acts against this accumulation of H^+ and subsequent triiodide formation. Therefore, the segregation index decreases and micromixing efficiency increases as the stirring speed increases.

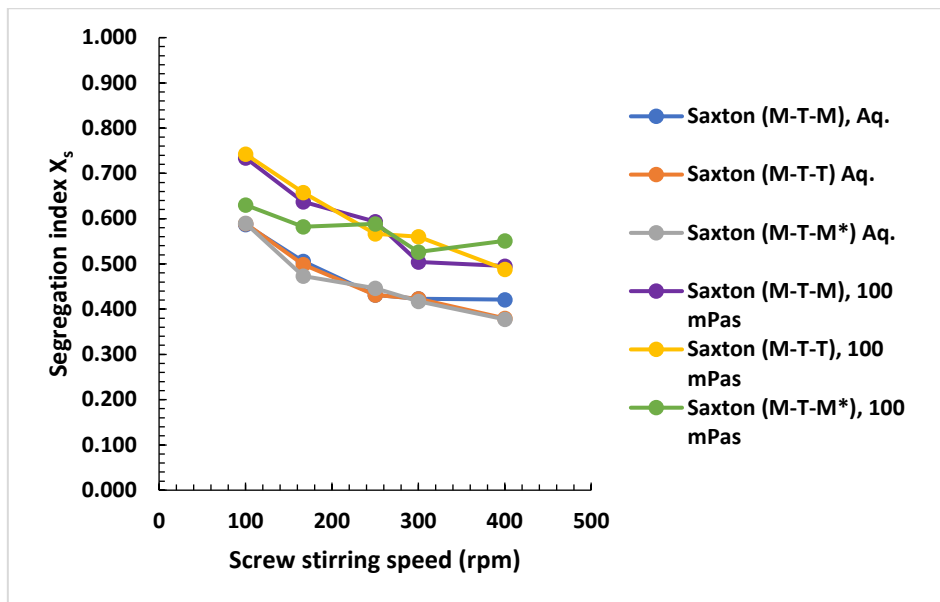


Figure 23: Effect of screw configuration on micromixing efficiency. M = Saxton mixing element and M^* is Normal pin mixing element. Mixing element M is closest to the reactor inlet. Each datapoint was measured once, $n = 1$

4.2.4 Sub-conclusion

The flow experiments show that micromixing in the screw is most efficient if aqueous solutions are mixed and Saxton mixing elements are implemented. The segregation index is independent of used screw configuration because the Villermaux-Dushman reactions are nearly instantaneous which makes the use multiple mixing elements obsolete. Furthermore, a combination of different mixing elements namely “Inlet-Saxton-Transport-Normal pin-Outlet” showed that the first mixing element that the fluid encounters is decisive for micromixing efficiency.

5 Conclusion

The goal of this thesis was to characterize micromixing in batch and screw reactors. Batch experiments served as a benchmark to gauge if the Villermaux-Dushman method was viable in higher viscous systems. Critical injection times and stirring speed sweeps were done for both aqueous and 100 mPa·s solutions. The used batch reactor is therefore characterized within the used parameter ranges. The characterization of micromixing in the screw reactor was the primary objective of this thesis and required an investigation into the effects of stirring speed, viscosity, mixing element type, and screw configuration. For viscosity 1 mPa·s and 100 mPa·s and within the stirring speed range used, micromixing has been characterized in the used screw reactor. This thesis shows that micromixing is more efficient in aqueous solution for both a batch and a single-screw extrusion reactor. Secondly, Saxton mixing elements enhance micromixing the most, independent of the viscosity of the solution. Additionally, screw configuration was found to have no significant effect on micromixing efficiency. Only the first mixing element that the fluid encounters is decisive for micromixing efficiency because the Villermaux-Dushman reactions are nearly instantaneous.

However, only Normal pin and Saxton mixing elements were investigated in this thesis, future research could focus on other mixing element types, for example, Dulmage and Pineapple pin mixing elements. Another objective for future research is expanding the viscosity range up to 1 Pas or even 10 Pas. The use of glycerol as the viscosifying agent is discouraged because of the amount of glycerol that would be needed to achieve viscosities greater than 100 mPa·s. To optimize the use versus cost, a replacement for glycerol should be found. This viscosifying agent is preferably cheaper relative to glycerol but also should have greater viscosifying power which means that less product is needed to gain an arbitrary viscosity compared to glycerol. Additionally, an alternative viscosifying agent preferably does not introduce interfering agents, for example, premature discoloration of the buffer solution. Moreover, the maximal screw stirring speed was limited to 400 rpm. In future research this range could be expanded upon however this would require a different motor or a different gear ratio which is 3:1 (motor: screw) for this thesis.

Furthermore, the data obtained from batch experiments were prone to significant variations specifically for 100 mPa·s solutions which could be due to improper sampling or air bubbles. Therefore, inline measuring should be considered. Lastly, batch and screw reactors were not compared directly in this thesis although an in-depth comparison of micromixing efficiency between these reactors is possible through calculation and comparison of micromixing times (t_{micro}). This calculation is another possible next step for future research. Evidently, all the experiments done in this thesis can be repeated many times to achieve more data points and make a model.

References

- [1] "CIPT." Accessed: Mar. 16, 2024. [Online]. Available: <https://iiw.kuleuven.be/onderzoek/cipt/about-cipt>
- [2] G. Nagendrappa, "Organic Synthesis under Solvent-free Condition. An Environmentally Benign Procedure - I," *RESONANCE*, Oct. 2002.
- [3] S. B. Aljuboori, N. A. Abdulrahim, S. Yassen, and H. H. Khaleel, "Solvent Role in Organic Chemistry in Comparison with Organic Synthesis under Solvent-Free Condition (Green Chemistry): A Mini Literature Review," *Al-Rafidain Journal of Medical Sciences*, vol. 3. Al-Rafidain University College, pp. 109–115, Jul. 01, 2022. doi: 10.54133/ajms.v3i.94.
- [4] M. Himaja, P. Das, and Karigar A., "GREEN TECHNIQUE - SOLVENT FREE SYNTHESIS AND ITS ADVANTAGES," *Int J Res Ayurveda Pharm*, vol. 2, no. 4, pp. 1079–1086, 2011.
- [5] R. R. A. Bolt, J. A. Leitch, A. C. Jones, W. I. Nicholson, and D. L. Browne, "Continuous flow mechanochemistry: reactive extrusion as an enabling technology in organic synthesis," *Chemical Society Reviews*, vol. 51, no. 11. Royal Society of Chemistry, pp. 4243–4260, May 04, 2022. doi: 10.1039/d1cs00657f.
- [6] J. Loncke, "Project Outline - PhD," KULeuven, Diepenbeek. Accessed: Apr. 22, 2024. [Online]. Available: <https://onedrive.live.com/edit.aspx?resid=22FA64D9F2580E62!357&cid=22fa64d9f2580e62&CT=1713786290548&OR=ItemsView>
- [7] S. L. James *et al.*, "Mechanochemistry: new and cleaner synthesis Author list, addresses and affiliations."
- [8] J. L. Howard, Y. Sagatov, L. Repousseau, C. Schotten, and D. L. Browne, "Controlling Reactivity Through Liquid Assisted Grinding: The Curious Case of Mechanochemical Fluorination," in *AICHe Annual Meeting, Conference Proceedings*, American Institute of Chemical Engineers, 2019. doi: 10.1039/x0xx00000x.
- [9] D. E. Crawford, C. K. Miskimmin, J. Cahir, and S. L. James, "Continuous multi-step synthesis by extrusion-telescoping solvent-free reactions for greater efficiency," *Chemical Communications*, vol. 53, no. 97, pp. 13067–13070, 2017, doi: 10.1039/c7cc06010f.
- [10] P. Ying, J. Yu, and W. Su, "Liquid-Assisted Grinding Mechanochemistry in the Synthesis of Pharmaceuticals," *Advanced Synthesis and Catalysis*, vol. 363, no. 5. Wiley-VCH Verlag, pp. 1246–1271, Mar. 02, 2021. doi: 10.1002/adsc.202001245.
- [11] "Single Screw Extruder VS Twin Screw Extruder - Kairong Machinery." Accessed: Apr. 22, 2024. [Online]. Available: <https://www.kaironggroup.com/single-screw-extruder-vs-twin-screw-extruder/>
- [12] D. E. Crawford, "Extrusion - Back to the future: Using an established technique to reform automated chemical synthesis," *Beilstein Journal of Organic Chemistry*, vol. 13. Beilstein-Institut Zur Forderung der Chemischen Wissenschaften, pp. 65–75, Jan. 11, 2017. doi: 10.3762/bjoc.13.9.
- [13] E. Colacino *et al.*, "Mechanochemistry for 'no solvent, no base' preparation of hydantoin-based active pharmaceutical ingredients: Nitrofurantoin and dantrolene," *Green Chemistry*, vol. 20, no. 13, pp. 2973–2977, 2018, doi: 10.1039/c8gc01345d.
- [14] B. M. Sharma, R. S. Atapalkar, and A. A. Kulkarni, "Continuous flow solvent free organic synthesis involving solids (reactants/products) using a screw reactor," *Green Chemistry*, vol. 21, no. 20, pp. 5639–5646, 2019, doi: 10.1039/c9gc02447f.
- [15] D. Crawford, J. Casaban, R. Haydon, N. Giri, T. McNally, and S. L. James, "Synthesis by extrusion: Continuous, large-scale preparation of MOFs using little or no solvent," *Chem Sci*, vol. 6, no. 3, pp. 1645–1649, Mar. 2015, doi: 10.1039/c4sc03217a.
- [16] E. L. Paul, H. Mahadevau, J. Foster, M. Kennedy, and M. Mid&, "THE EFFECT OF MIXING ON SCALEUP OF A PARALLEL REACTION SYSTEM," 1992.

- [17] J. Baldyga, J. R. Bourne', and Y. Yang', "INFLUENCE OF FEED PIPE DIAMETER ON MESOMIXING IN STIRRED TANK REACTORS," 1993.
- [18] J. Bałdyga, M. Henczka, and Makowski, "Effects of mixing on parallel chemical reactions in a continuous-flow stirred-tank reactor," *Chemical Engineering Research and Design*, vol. 79, no. 8, pp. 895–900, 2001, doi: 10.1205/02638760152721109.
- [19] S. Al-Hengari and B. Sc, "Process Intensification: A Study of Micromixing and Residence Time Distribution Characteristics in the Spinning Disc Reactor by," 2011.
- [20] A. Rozeń, R. A. Bakker, and J. Bałdyga, "Effect of operating parameters and screw geometry on micromixing in a co-rotating twin-screw extruder," *Chemical Engineering Research and Design*, vol. 79, no. 8, pp. 938–942, 2001, doi: 10.1205/02638760152721163.
- [21] J. M. Commenge and L. Falk, "Villermaux-Dushman protocol for experimental characterization of micromixers," *Chemical Engineering and Processing: Process Intensification*, vol. 50, no. 10, pp. 979–990, Oct. 2011, doi: 10.1016/j.cep.2011.06.006.
- [22] V. Hessel, S. Hardt, H. Lowe, F. Schönfeld", and S. Schönfeld", "Laminar Mixing in Different Interdigital Micromixers: I. Experimental Characterization."
- [23] F. Schönfeld, V. Hessel, and C. Hofmann, "An optimised split-and-recombine micro-mixer with uniform 'chaotic' mixing," *Lab Chip*, vol. 4, no. 1, pp. 65–69, 2004, doi: 10.1039/b310802c.
- [24] T. Kirner, J. Albert, M. Günther, G. Mayer, K. Reinhäkel, and J. M. Köhler, "Static micromixers for modular chip reactor arrangements in two-step reactions and photochemical activated processes," *Chemical Engineering Journal*, vol. 101, no. 1–3, pp. 65–74, Aug. 2004, doi: 10.1016/j.cej.2003.10.029.
- [25] S. H. Wong, M. C. L. Ward, and C. W. Wharton, "Micro T-mixer as a rapid mixing micromixer," *Sens Actuators B Chem*, vol. 100, no. 3, pp. 359–379, May 2004, doi: 10.1016/j.snb.2004.02.008.
- [26] P. Guichardon and L. Falk, "Characterisation of micromixing efficiency by the iodide-iodate reaction system. Part I: Experimental procedure," *Chem Eng Sci*, vol. 55, no. 19, pp. 4233–4243, 2000, doi: 10.1016/S0009-2509(00)00068-3.
- [27] J. Pinot, J. M. Commenge, J. F. Portha, and L. Falk, "New protocol of the Villermaux-Dushman reaction system to characterize micromixing effect in viscous media," *Chem Eng Sci*, vol. 118, pp. 94–101, Oct. 2014, doi: 10.1016/j.ces.2014.07.010.
- [28] E. Arian and W. Pauer, "Sucrose solution as a new viscous test fluid with tunable viscosities up to 2 Pas for micromixing characterization by the Villermaux–Dushman reaction," *J Flow Chem*, vol. 11, no. 3, pp. 579–588, Sep. 2021, doi: 10.1007/s41981-021-00158-1.
- [29] M.-C. Fournier, L. Falk, and J. Villermaux, "A NEW PARALLEL COMPETING REACTION SYSTEM FOR ASSESSING MICROMIXING EFFICIENCY-EXPERIMENTAL APPROACH," 1996.
- [30] S. Ehlers, K. Elgeti, T. Menzel, and G. Wießmeier, "Mixing in the offstream of a microchannel system," 2000. [Online]. Available: www.elsevier.com/locate/cep
- [31] K. J. Hecht, A. Kölbl, M. Kraut, and K. Schubert, "Micromixer characterization with competitive-consecutive bromination of 1,3,5-trimethoxybenzene," *Chem Eng Technol*, vol. 31, no. 8, pp. 1176–1181, Aug. 2008, doi: 10.1002/ceat.200800213.
- [32] L. Camps, L. Moens, U. Groth, L. Braeken, S. Kuhn, and L. C. J. Thomassen, "Batch reactor scale-up of the mixing-sensitive Bechamp reaction based on the heat pulse method."
- [33] D. A. Palmer, R. W. Ramette, and R. E. Mesmer, "Triiodide ion formation equilibrium and activity coefficients in aqueous solution," *J Solution Chem*, vol. 13, no. 9, pp. 673–683, Sep. 1984, doi: 10.1007/BF00650374.
- [34] J. Villermaux, "MACRO AND MICROMIXING PHENOMENA IN CHEMICAL REACTORS," 1984.
- [35] S. R. L. Gobert, S. Kuhn, L. Braeken, and L. C. J. Thomassen, "Characterization of Milli- and Microflow Reactors: Mixing Efficiency and Residence Time Distribution," *Org Process Res Dev*, vol. 21, no. 4, pp. 531–542, Apr. 2017, doi: 10.1021/acs.oprd.6b00359.

- [36] K. Kunowa, S. Schmidt-Lehr, W. Pauer, H. U. Moritz, and C. Schwede, "Characterization of mixing efficiency in polymerization reactors using competitive-parallel reactions," in *Macromolecular Symposia*, 2007, pp. 32–41. doi: 10.1002/masy.200751305.
- [37] L. Nouri, J. Legrand, N. Benmalek, F. Imerzoukene, A. R. Yeddou, and F. Halet, "Characterisation and comparison of the micromixing efficiency in torus and batch stirred reactors," *Chemical Engineering Journal*, vol. 142, no. 1, pp. 78–86, Aug. 2008, doi: 10.1016/j.cej.2008.01.030.
- [38] W. Dolshanskiy, A. Stepanyuk, E. Arian, and W. Pauer, "Residence time distribution and micromixing efficiency of a dynamic inline rotor–stator mixer," *Chemical Engineering Journal*, vol. 451, Jan. 2023, doi: 10.1016/j.cej.2022.138555.
- [39] M. Assirelli, S. P. Lee, and A. W. Nienow, "Further Studies of Micromixing: Scale-Up, Baffling and Feed Pipe Backmixing," *Journal of Chemical Engineering of Japan*, vol. 44, no. 11, pp. 901–907, 2011.
- [40] S. H. Jung, J. W. Yeon, Y. Kang, and K. Song, "Determination of triiodide ion concentration using UV-visible spectrophotometry," in *Asian Journal of Chemistry*, Chemical Publishing Co., 2014, pp. 4084–4086. doi: 10.14233/ajchem.2014.17720.
- [41] P. Guichardon, L. Falk, and J. Villermaux, "Extension of a chemical method for the study of micromixing process in viscous media," 1997.
- [42] K. M. Van Geem, G. J. Heynderickx, Y. Ouyang, M. Nunez Manzano, and K. Beirnaert, "Micromixing in a gas-liquid vortex reactor," *AIChE Journal*, vol. 67, no. 7, Jan. 2021, doi: 10.1002/aic.17064.
- [43] F. Zhang, S. Marre, and A. Erriguible, "Mixing intensification under turbulent conditions in a high pressure microreactor," *Chemical Engineering Journal*, vol. 382, Feb. 2020, doi: 10.1016/j.cej.2019.122859.
- [44] D. C. Wilcox, *Turbulence modeling for CFD*, 3rd ed., vol. 3. DCW Industries, 2006.